frontiers in
NEUROANATOMY

ORIGINAL RESEARCH ARTICLE
published: 22 August 2011
doi: 10.3389/fnana.2011.00054

Amygdaloid projections to the ventral striatum in mice: direct and indirect chemosensory inputs to the brain reward system

Amparo Novejarque[1†], Nicolás Gutiérrez-Castellanos[2†], Enrique Lanuza[2]* and Fernando Martínez-García[1]*

[1] *Departament de Biologia Funcional i Antropologia Física, Facultat de Ciències Biològiques, Universitat de València, València, Spain*
[2] *Departament de Biologia Cel•lular, Facultat de Ciències Biològiques, Universitat de València, València, Spain*

Edited by:
Agustín González, Universidad Complutense de Madrid, Spain

Reviewed by:
Daniel W. Wesson, Case Western Reserve University, USA
James L. Goodson, Indiana University, USA

****Correspondence:***
Enrique Lanuza, Departament de Biologia Cel•lular, Facultat de Ciències Biològiques, Universitat de València, C/Dr. Moliner, 50 ES-46100 Burjassot, València, Spain.
e-mail: enrique.lanuza@uv.es;
Fernando Martínez-García, Departament de Biologia Funcional i Antropologia Física, Facultat de Ciències Biològiques, Universitat de València, C/Dr. Moliner, 50 ES-46100 Burjassot, València, Spain.
e-mail: fernando.mtnez-garcia@uv.es

†Present address:
Amparo Novejarque, Department of Surgery and Cancer, Faculty of Medicine, Imperial College London, Chelsea and Westminster Hospital, London, UK;
Nicolás Gutiérrez-Castellanos, Cerebellar coordination and cognition group, Netherlands Institute for Neuroscience, Amsterdam, Netherlands.

Rodents constitute good models for studying the neural basis of sociosexual behavior. Recent findings in mice have revealed the molecular identity of the some pheromonal molecules triggering intersexual attraction. However, the neural pathways mediating this basic sociosexual behavior remain elusive. Since previous work indicates that the dopaminergic tegmento-striatal pathway is not involved in pheromone reward, the present report explores alternative pathways linking the vomeronasal system with the tegmento-striatal system (the limbic basal ganglia) by means of tract-tracing experiments studying direct and indirect projections from the chemosensory amygdala to the ventral striato-pallidum. Amygdaloid projections to the nucleus accumbens, olfactory tubercle, and adjoining structures are studied by analyzing the retrograde transport in the amygdala from dextran amine and fluorogold injections in the ventral striatum, as well as the anterograde labeling found in the ventral striato-pallidum after dextran amine injections in the amygdala. This combination of anterograde and retrograde tracing experiments reveals direct projections from the vomeronasal cortex to the ventral striato-pallidum, as well as indirect projections through different nuclei of the basolateral amygdala. Direct projections innervate mainly the olfactory tubercle and the islands of Calleja, whereas indirect projections are more widespread and reach the same structures and the shell and core of nucleus accumbens. These pathways are likely to mediate innate responses to pheromones (direct projections) and conditioned responses to associated chemosensory and non-chemosensory stimuli (indirect projections). Comparative studies indicate that similar connections are present in all the studied amniote vertebrates and might constitute the basic circuitry for emotional responses to conspecifics in most vertebrates, including humans.

Keywords: chemosensory amygdala, nucleus accumbens, olfactory tubercle, islands of Calleja, striatal cell bridges, emotional brain

INTRODUCTION

It is generally accepted that the amygdala is a key structure in the generation of emotional behaviors (LeDoux, 2000). Remarkably, in this view of the amygdala as the core of the emotional brain, its chemosensory role is usually neglected (see Aggleton, 2000), despite the fact that one of the major sensory inputs to the amygdala originates in the main and accessory olfactory bulbs, providing directly olfactory and vomeronasal information (Pitkänen, 2000). Chemosensory stimuli have a strong influence on the behavior of rodents, in particular in sociosexual behaviors

Abbreviations: AA, anterior amygdaloid area (AAD: dorsal; AAV: ventral); AB, accessory basal (or basomedial) amygdaloid nucleus (ABa: anterior; ABp: posterior); *ac*, anterior commissure (*aca*: anterior part; *acp*: posterior part); Acb, nucleus accumbens (AcbC: core; AcbSh: shell; LAcbSh: lateral shell; MAcbSh: medial shell); AHA, amygdalohippocampal area (AHAl: lateral division; AHAm: medial division); APir, amygdalopiriform transition area; AStr, amygdalo-striatal transition area; B, basal (or basolateral) amygdaloid nucleus (Ba: anterior; Bp: posterior; Bv: ventral); BAOT, bed nucleus of the accessory olfactory tract; BST, bed nucleus of the *stria terminalis*; CB, cell bridges of the ventral striatum; Ce, central amygdaloid nucleus (CeC: capsular or paracapsular division; CeL: lateral division; CeM: medial division); Cl, claustrum; COAa, anterior cortical amygdaloid nucleus; COApl, posterolateral cortical amygdaloid nucleus; COApm, posteromedial cortical amygdaloid nucleus; CPu, caudate–putamen (dorsal striatum); CxA, cortex–amygdala transition zone; DEn, dorsal endopiriform nucleus; HDB, horizontal limb of the diagonal band nucleus; I, intercalated nuclei of amygdala; ICj, islands of Calleja; ICjM, major island of Calleja; IPAC, interstitial nucleus of the posterior limb of the anterior commissure; L, lateral amygdaloid nucleus (Lvl: ventrolateral, Ldl: dorsolateral, Lm: medial); LGP, lateral globus pallidus; LOT, nucleus of the lateral olfactory tract (1: layer 1; 2: layer 2; 3: layer 3); Me, medial amygdaloid nucleus; MeA, anterior medial amygdala; MeP, posterior medial amygdala (MePV: ventral; MePD: dorsal); Pir, piriform cortex; SI, *substantia innominata*; *st, stria terminalis*; Tu, olfactory tubercle; VEn, ventral endopiriform nucleus.

having an important emotional component. In this respect, recent findings in mice have uncovered the molecular identity of two particular pheromonal molecules triggering intersexual attraction (Roberts et al., 2010) and sexual receptivity (Haga et al., 2010). Male-soiled bedding containing some of these pheromones can be used to induce conditioned place preference (Martínez-Ricós et al., 2007) and, therefore, these sexual pheromones should be considered rewarding stimuli. Since the major pathway involved in reward processing is the dopaminergic tegmento-striatal pathway, our group has previously analyzed the role of this projection in pheromonal reward in mice. Neither systemic administration of anti-dopaminergic drugs (Agustín-Pavón et al., 2007), nor lesions of the dopaminergic neurons of the ventral tegmental area (Martínez-Hernández et al., 2006) abolish female preference for male-soiled bedding, thus suggesting that the dopaminergic tegmento-striatal pathway is not involved in pheromone reward.

In mice, at least some male sexual pheromones attractive for females are detected by the vomeronasal system (Martínez-Ricós et al., 2008), and consequently information about these sexual pheromones is processed in the vomeronasal amygdala. There is increasing evidence on the role of the amygdala on reward-related processes (Baxter and Murray, 2002; Everitt et al., 2003), but the role of the amygdala in reward driven by chemosensory stimuli has been rarely explored. The pioneering studies by Everitt, Robbins, and collaborators (Cador et al., 1989; Everitt et al., 1989, 1991; Robbins et al., 1989) indicated that basolateral amygdala projections to the nucleus accumbens mediate reward-related learning. In contrast, much less information is available regarding the projections from the chemosensory amygdala to the nucleus accumbens and other centers of the ventral striatum (McDonald, 1991b; Canteras et al., 1992; Shammah-Lagnado and Santiago, 1999).

The present report explores alternative pathways linking the chemosensory amygdala with the brain reward system by means of tract-tracing experiments studying the projections of different amygdaloid nuclei to the ventral striato-pallidum. To do so, we combine anterograde and retrograde tracing experiments to reveal amygdaloid projections to the nucleus accumbens, olfactory tubercle, and adjoining structures such as the islands of Calleja (ICj). Our results might help to understand the neural pathways mediating the behavioral responses to chemical cues, including rewarding sexual pheromones.

MATERIALS AND METHODS

ANIMALS

For this study, 35 adult, female mice (*Mus musculus*, Harlan, Barcelona, Spain; 25 of the C57BL/J6 strain and 10 of the CD1 strain) were used (17.9–35.1 g). Animals were maintained in cages with food and water *ad libitum*, under natural day/night cycle, at 22–25°C. All experiments were performed in accordance with the guidelines of the European Community Council Directive 86/609/EEC on the treatment of experimental animals, and procedures were approved by the Committee of Ethics on Animal Experimentation of the University of València.

TRACT-TRACING EXPERIMENTS

To study the amygdaloid projections to the ventral striatum in the mouse, we first injected neuroanatomical tracers in different parts of the Acb (medial shell, $n = 4$; lateral shell, $n = 1$; core, $n = 5$; non-restricted injections, $n = 2$) and other regions of the ventral striatum [olfactory tubercle, $n = 6$; major island of calleja (ICjM), $n = 1$], to study the distribution of retrograde labeling in the amygdala. Then, tracers were injected in the different nuclei of the amygdala that showed retrograde labeling in the previous experiments (cortical amygdala, $n = 7$; deep pallial amygdala, $n = 10$) and the resulting anterograde labeling in the ventral striatum was analyzed. In order to study whether the associative nuclei of the deep pallial amygdala (lateral, basal and accessory basal) can indirectly relay chemosensory information to the ventral striatum, we also studied the intra-amygdaloid projections from the cortical (chemosensory) amygdaloid nuclei to the deep pallial amygdala.

In the present work, three different tracers were used: biotinylated dextran amine (BDA, 10,000 and 3,000 MW lysine fixable; Invitrogen, Carlsbad, CA, USA), tetramethylrhodamine-labeled dextran amine (RDA, 10,000 MW, lysine fixable, fluoro-ruby; Invitrogen) and fluorogold (Biotium, Hayward, CA, USA). To minimize the number of animals, each mouse usually received two tracer injections (total number of tracer injections, 46). Therefore, each injection is identified with a letter indicative of the tracer (B for BDA; R for RDA; F for fluorogold) and a number indicative of the specimen.

For surgery, animals were deeply anesthetized with an intraperitoneal injection of 6.5 µl of sodium pentobarbital (11 mg/ml, Sigma-Aldrich, St. Louis, MO, USA) per gram of body weight. Using stereotaxic coordinates (Paxinos and Franklin, 2001), dextran amines (5–10% in 0.01 M phosphate buffer, pH 7.6), and fluorogold (2% in saline solution) were ionophoretically injected through glass micropipettes with an inner diameter tip of 10–20 µm, using positive current (7 s on/off; 3–5 µA) during 10 min. The pipette was left in place for 5 min after injection. To avoid diffusion of the tracer along the pipette track, a mild continuous retention current (−0.9 µA) was applied during entrance and withdrawal of the micropipette. After 7–8 days of survival, animals received an overdose of sodium pentobarbital and were perfused transcardially with phosphate buffered saline (PBS; 0.9% NaCl in 0.1 M PB pH 7.6), followed by fixative (4% paraformaldehyde in 0.1 M PB, pH 7.6). Brains were postfixed for 4 h in the same fixative at 4°C and then immersed in 30% sucrose in 0.1 M PB until they sank. Frontal sections (40 µm) obtained with a freezing microtome were collected into five parallel series.

Before (immuno)histochemical processing, endogenous peroxidase was inhibited with 1% H_2O_2 in 0.05 M TRIS buffer (TB) pH 7.6 plus 0.9% NaCl (TRIS-buffered saline, TBS) for 30 min at room temperature. For BDA detection, sections were incubated in avidin–biotin complex (ABC Elite kit; Vector Laboratories, Burlingame, CA, USA) in TBS with 0.3% Triton X-100, either overnight at 4°C or for 2 h at room temperature, and then the peroxidase activity was revealed with 3,3′-diaminobenzidine (DAB, Sigma; 0.02% in 0.05 M TB, pH 7.6–8.0) and 0.01% H_2O_2. Nickel salts (0.4% nickel ammonium sulfate) were added as an enhancing agent of the reaction product (DAB-Ni).

For immunodetection of tetramethyl rhodamine, sections were incubated in primary antibody against tetramethyl rhodamine (raised in rabbit, Molecular Probes, Cat. # A-6397, Lot: 7051-3), diluted 1:4,000 in TBS with 0.3% Triton X-100, followed by a standard peroxidase–antiperoxidase procedure (goat anti-rabbit IgG,1:100, Nordic Immunological Laboratories, Tilburg, The Netherlands; rabbit PAP, 1:800, Nordic Immunological Labs). The resulting peroxidase label was revealed as above, with or without nickel enhancement.

Fluorogold injections were observed with fluorescence microscopy. Some series were also processed for the immunohistochemical detection of the tracer. To do so, sections were postfixed with 0.1% glutaraldehyde in PBS for 4 h at 4°C, rinsed in TBS and the endogenous peroxidase activity was inhibited with 1% H_2O_2 (30 min). Sections were then sequentially incubated in primary antibody (rabbit anti-FG, Chemicon, Billerica, MA, USA) diluted 1:5,000 in TBS with 0.3% Triton X-100 and 2.5% normal goat serum, overnight at 4°C; secondary antibody (biotinylated goat anti-rabbit IgG, Vector Laboratories, Burlingame, CA, USA) diluted 1:200 in TBS-Tx for 2 h at room temperature; and ABC Elite (2 h, room temperature, Vector Labs) diluted in the same buffer. The resulting peroxidase labeling was visualized as detailed above.

IMAGE ACQUISITION AND PROCESSING

Slides were photographed in a Leitz DMRB microscope equipped with a Leica DC 300 digital camera (Leica Microsystems, Wetzlar, Germany). Digital images were imported into Adobe Photoshop (Adobe Systems, Mountain View, CA, USA), flattened by subtracting background illumination and converted to gray scale. Brightness and contrast were adjusted and resolution was set at 600 dpi. No additional filtering or manipulation of the images was performed. The final figures were composed and labeled with Adobe Photoshop.

Chartings of anterograde labeling in specific sections were drawn for illustration purposes. To do so, low-power photomicrographs of the sections were taken as described and two transparent sheets were created on top of them using Adobe Photoshop. One of them was used to delineate the cytoarchitecture of the section, whereas in the other one a detailed map of the labeling was drawn using some elements of the photograph as spatial landmarks (vessels, ventricles, Nissl staining, etc.) while observing the slides at high magnification through the microscope.

RESULTS

The results of our experiments are described following the nomenclature by Paxinos and Franklin (2001), except for the amygdala, where we have partially adapted the nomenclature of Pitkänen (2000). This terminology has the advantage of avoiding the confusion between the basolateral nucleus and the basolateral division of the amygdala. Briefly, the amygdala consists of a mixture of structures with pallial or subpallial origin (Puelles et al., 2000; see **Figure 1**). The pallial structures of the amygdala give rise to the bulk of the amygdalo-striatal projections, and therefore are the focus of the present investigation. Within the pallial amygdala, we distinguish the cortical nuclei (superficial, olfacto-recipient, and layered) and several non-layered nuclei located topologically deep to them (**Figure 1**). The cortical nuclei include the nucleus of the lateral olfactory tract (LOT, **Figure 1A,A′**), the anterior cortical amygdaloid nucleus (COAa, **Figure 1A–B′**), the posterolateral cortical amygdaloid nucleus (COApl, **Figure 1B–D′**), as well as of two secondary vomeronasal centers, the bed nucleus of the accessory olfactory tract (BAOT, not shown) and the posteromedial cortical amygdaloid nucleus (COApm, **Figure 1C–D′**). In addition, there are several transitional areas interposed between the cortical amygdala and the piriform cortex (cortex–amygdala transition zone,

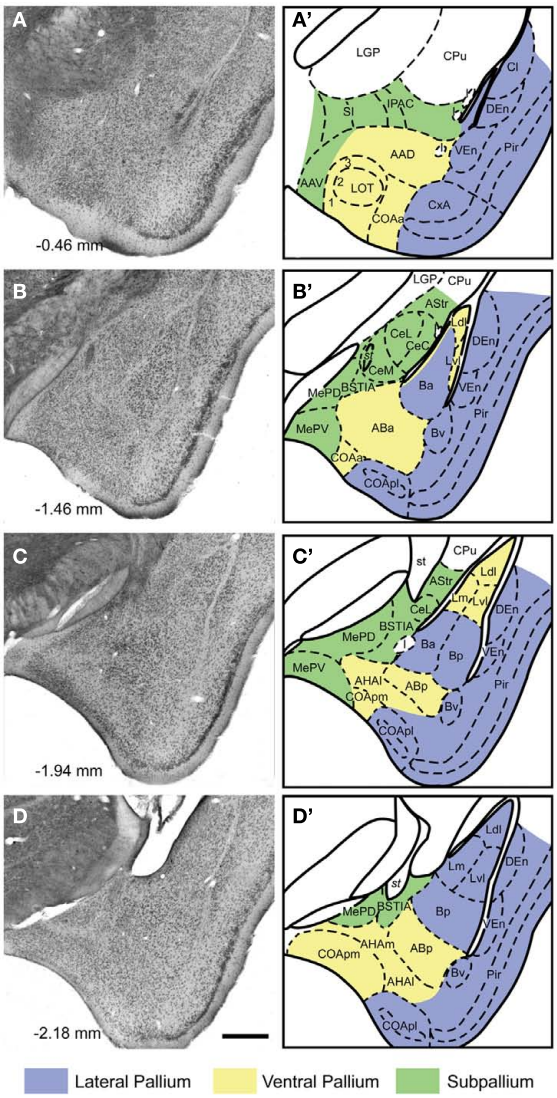

FIGURE 1 | Cytoarchitecture of the amygdaloid complex of the mouse Nissl-stained frontal sections (A–D) through the amygdala of the mouse (A rostral, D caudal) with indication of the antero-posterior level relative to Bregma according to Paxinos and Franklin (2001). In the right panels **(A′–D′)**, the boundaries between the different nuclei and fiber tracts are delineated in schematic drawings of the same sections. The embryological origin (subpallial, lateropallial, ventropallial) of the different amygdaloid structures is also indicated. For abbreviations, see list. Calibration bar = 400 μm.

CxA, **Figure 1A,A′**; amygdalopiriform transition area, APir, not shown). The deep pallial nuclei of the amygdala include the basal (B, or basolateral, **Figure 1B–D′**), the accessory basal (AB, or basomedial, **Figure 1B–D′**), and the lateral (L, **Figure 1B–D′**) amygdaloid nuclei, as well as the amygdalohippocampal area (AHA, **Figure 1C–D′**). According to Paxinos and Franklin (2001), we consider that the B includes anterior (Ba), posterior (Bp), and ventral (Bv) divisions. Within the AB we distinguish anterior (ABa) and posterior (ABp) portions. The L shows ventrolateral (Lvl), dorsolateral (Ldl), and medial (Lm) divisions. Finally, within the AHA we consider medial (AHAm) and lateral (AHAl) subnuclei.

In the ventral striatum we consider the core (AcbC) and shell (AcbSh) of the nucleus accumbens (with its lateral and medial divisions; LAcbSh and MAcbSh respectively) following Paxinos and Franklin (2001). We also include the olfactory tubercle (Tu), the ICj, and the cell bridges of the ventral striatum (CB) since the anterograde labeling in nucleus accumbens after injections in the pallial amygdala was continuous with the one found in these structures (for previous descriptions of the striatal cell bridges in the rat see Seifert et al., 1998; Riedel et al., 2002).

RETROGRADE LABELING ANALYSIS

Retrograde labeling in the amygdala after injections in the nucleus accumbens

We describe in detail the retrograde labeling of representative cases of tracer injections in the Acb (see **Table 1**). Remarkably, all of these injections gave rise to retrograde labeling in the cortical and deep pallial amygdala (see below). In contrast, retrogradely labeled cells were not observed in the central or the medial amygdaloid nuclei (with the exception of one injection involving part of the ventral septum, which gave rise to retrograde labeling in the medial amygdala, see Caffé et al., 1987).

Injections in the accumbens shell. Injections encompassing the MAcbSh rendered retrograde labeling in both the cortical and deep pallial amygdala (see **Table 1**). After these injections (**Figure 2A**), the cortical amygdala displayed a few labeled cells in the deep, lateral edge between the COAa and the CxA (**Figure 2B**) and in the caudal APir (**Figure 2E**). Injections including the rostral edge of the MAcbSh (R0304 and R0301) displayed few labeled neurons in the deep COApm (**Table 1**; **Figure 2E**). Within the deep pallial amygdala retrograde labeling was abundant in the whole B, including an area ventral to the Ba which we tentatively

Table 1 | Retrogradely labeled neurons in the different areas of the pallial amygdala (columns) after injections in the ventral striatum (rows) graded semi-quantitatively according to the following scores: –, absent; X, scarce; XX, moderate; XXX, dense; B, contralateral labeling.

	Cortical amygdala						Deep pallial amygdala									
	COApm	**LOT**	**COAa**	**CxA**	**COApl**	**APir**	**Ba**	**Bp**	**Bv**	**ABa**	***ABp***	**AHAl**	**AHAm**	**Lm**	**Lvl**	**Ldl**
ACCUMBENS SHELL																
R0304 MAcbSh +1.34 mm	X	–	X	–	–	X	XX	XXX B	XX	–	X	X	X	–	–	–
B0419 MAcbSh +0.98 mm	–	–	X	–	–	X	XXX	XXX	XX	–	XX	X	X	–	–	–
R0331 LAcbSh +1.10 mm	–	XX	X	XX	–	X	XXX B	XX	XX	–	XX	X	–	–	XX	–
ACCUMBENS CORE																
B0302 AcbC from +1.34 to +1.10 mm	–	X B	X	X	–	–	XX B	X	XX B	–	XXX B	X B	–	–	X	XXX B
B0309 dorsomedialAcbC +1.18 mm	–	X	–	X	–	–	X	X	–	–	X	–	–	–	–	X
B0321 lateralAcbC +1.18 mm	–	X	–	–	–	–	XX	X	X	–	X	–	–	–	X	XX
OLFACTORY TUBERCLE																
F08100 ICj anteromedial +0.98 mm	XX	XX	XX	X	XX	XX	–	XXX B	X	XX	XXX B	XX	X	–	–	–
NON-RESTRICTED INJECTIONS																
R0301 MAcbSh (+medial AcbC) +1.18 mm	X	–	X	–	–	X	XX	XXX B	XX	–	X B	X	X	–	X	–
R0338 dorsal MAcbSh + AcbC +0.98 mm	X	X	X	–	X	X	XX	XX B	XX	–	XX B	X B	XX	X	X	X
B0312 lateral S + ICjM from +1.34 to +1.10 mm	XXX	X B	X B	X	X	–	X	XX	–	XX B	X	XX	XX	–	X	–

The rostro-caudal extent of the injection site is indicated (coordinates from Bregma). For abbreviations, see list.

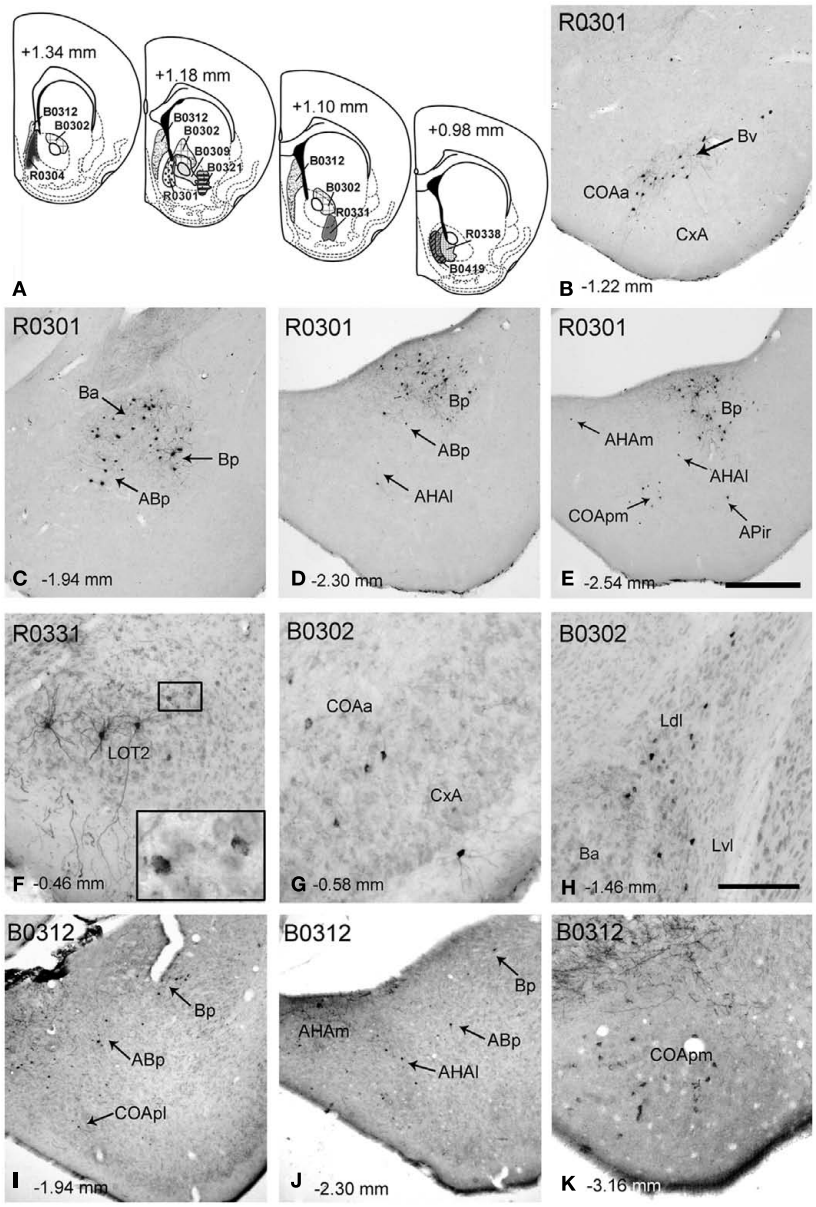

FIGURE 2 | Retrograde labeling in the pallial amygdala after tracer injections in the nucleus accumbens and associated major island of Calleja. (A) Semi-schematic drawings of coronal sections through the ventral striatum of the mouse showing the extent of tracer injections in the Acb and in the major island of Calleja. The antero-posterior coordinate relative to Bregma is indicated in each section as well as in every photograph in the figure. **(B–E)** Retrograde labeling in the pallial amygdala after an RDA injection encompassing the MAcbSh and a small portion of the medial AcbC (R0301). Although most of the labeling is located in the basolateral amygdala, retrogradely labeled cells are also present in deep layers of some cortical nuclei both in the anterior **(B,C)** and posterior amygdala **(D,E)**. **(F)** Retrogradely labeled neurons in the LOT ipsilateral to a tracer injection in the LAcbSh (R0331). Golgi-like labeled cells are clearly visible in layer 2, but layer 3 also displays cells showing granular labeling (inset). **(G,H)** Retrograde labeling in different centers of the pallial amygdala, resulting from a BDA injection in the AcbC (B0302). **(I–K)** Retrogradely labeled neurons in the pallial amygdala after a BDA injection in the ventral septum that encompassed the major island of Calleja (B0312). For abbreviations, see list. Calibration bar in **(E)** = 400 μm [also valid for **(B–D,I,J)**]. Scale bar in **(H)** = 150 μm [also valid for **(F–K)**].

consider as the Bv (**Figure 2B**). In addition, the caudal part of the Ba (**Figure 2C**) and the whole Bp (**Figures 2C–E**) showed many labeled somata. The most rostral injection in the MacbSh (R0304), as well as those injections involving both MAcbSh and AcbC (R0301 and R0338), rendered retrograde labeling in the contralateral Bp (**Table 1**). Moreover, retrogradely labeled cells were found in the posterior part of the AB (**Figures 1C,D**), where labeling was bilateral in the injections encompassing both the MAcbSh and AcbC (see **Table 1**). A few retrograde labeled cells were also present in the medial and lateral AHA (**Table 1**; **Figures 2D,E**). Finally, injections confined to the MAcbSh showed no labeled cells in the L (**Table 1**).

The injection in the lateral AcbSh (LAcbSh; R0331, **Figure 2A**) resulted in numerous labeled cells in several pallial amygdaloid centers. Within the cortical amygdala, labeled cells were abundant in the CxA but scarce in the COAa (see **Table 1**). At these rostral levels, the LOT showed Golgi-like labeled cells in layer 2 (**Figure 2F**), as well as a number of faintly labeled cell bodies in layer 3 (see inset in **Figure 2F**). At caudal levels, a few somata displayed granular retrograde labeling in the APir (not shown). In the deep pallial amygdala, labeled cells were abundant in all the subnuclei of the B, especially in the Ba, where labeling was bilateral with ipsilateral dominance (**Table 1**). The ABp also showed a moderate-to-high density of retrogradely labeled neurons (**Table 1**). A few labeled cells were also present in the AHAl (**Table 1**). Finally, a population of labeled neurons was confined to the rostral portion of the Lvl (**Table 1**).

Injections in the accumbens core. Two small injections restricted to the AcbC and a larger injection (B0302) including most of the dorsal AcbC plus a small portion of the adjacent caudate–putamen (**Figure 2A**) displayed scarce retrograde labeling (see **Table 1**) within the cortical amygdala. A few labeled cells were found bilaterally in layer 3 of the LOT (**Table 1**) and ipsilaterally in the CxA, especially in its deep portion, adjacent to the COAa (**Figure 2G**). On the other hand, the deep pallial amygdala showed a dense population of retrogradely labeled cells in the most anterior part of the L, especially dense in the Ldl, where labeling was bilateral. Labeled neurons were also observed in the Lvl (**Table 1**; **Figure 2H**). It is worth noting that this labeling was absent in the injections restricted to the MAcbSh. In addition, many retrogradely labeled neurons were observed in both hemispheres in the caudal aspect of the Ba (**Figure 2H**), in the Bv and in the AHAl. Moreover, some labeled neurons were observed in the rostralmost part of the Bp (not shown) and the ABp showed a dense population of retrogradely labeled cells (**Table 1**).

Injection involving the major island of Calleja. One injection centered in the lateral septum (B0312) extended ventrally to encompass the ICjM, which was the only structure in the ventral striatum affected by the injection (**Figure 2**). This injection gave rise to a high number of retrogradely labeled cells in different amygdaloid pallial centers (**Table 1**). All the nuclei in the cortical amygdala, with the exception of the APir, showed retrograde labeling (**Table 1**), the deep portion of the COApm (mainly its caudal aspect) being the nucleus with the highest density of labeled cells (**Figure 2K**). The COApl also showed some labeled somata in its most rostral and deep aspect (**Figure 2I**). Both the superficial COAa (bilaterally) and the medial CxA showed some labeled neurons (**Table 1**). The LOT also displayed neurons with granular labeling in the layer 2 bilaterally (not shown). In the deep pallial amygdala some neurons were present in the ventral and caudal end of the Ba and a moderate number of labeled cells in the Bp (**Figures 2I,J**). The AB showed some labeled neurons in the ventral region of the caudalmost ABa (bilaterally) and in the ABp (**Table 1**; **Figures 2I,J**). In the AHA the number of labeled cells was moderate in both subdivisions (**Figure 2J**). Finally, some neurons in the Lvl showed granular labeling (**Table 1**).

Retrograde labeling in the amygdala after injections in the olfactory tubercle

Fluorogold injections involved the olfactory tubercle in six occasions. Retrograde labeling in experiment F08100 is shown as representative example. In this case, the tracer injection was centered in the ventromedial aspect of the olfactory tubercle and encompassed the anteromedial ICj (**Figure 3A**). Retrogradely labeled neurons in the cortical amygdala appeared mainly in the LOT (**Table 1**), COAa (**Figure 3B**), COApm and COApl, (in all three structures located in layers 2 and 3), and in APir (**Figures 3C,D**). A number of labeled somata appeared also in CxA. Of note, labeled cells were also observed in the medial amygdala (subpallium), but only in its anterior part (**Figure 3B**). In the deep pallial amygdala, fluorogold-labeled cells were abundant in the AB (both anterior and posterior parts), B (posterior and ventral parts), and AHA (**Figures 3C,D**). In contrast, virtually no labeling was present in the Ba and very few cells were observed in the caudal L. Outside the amygdala, but worth mentioning given its olfactory nature, dense retrograde labeling was observed in the posterior aspect of the piriform cortex (**Figures 3C,D**).

ANTEROGRADE LABELING ANALYSIS

Anterograde labeling in the ventral striatum after injections in the cortical amygdala

Seven injections were aimed at the cortical portion of the pallial amygdala (**Figure 4**), six of which were centered in the caudal cortical amygdala whereas the other one encompassed the rostral CxA and the COAa (**Figure 4A**). The anterograde labeling observed in the ventral striatum in representative cases (see **Tables 2** and **3**) is described below.

Injections in the posterior cortical amygdala. Injections B0415 and R0341 involved, to different degrees, the COApm and COApl. Case B0415 was a large BDA injection, which mainly affected the COApm but also encompassed the medialmost aspect of the COApl. On the other hand, R0341 was quite a restricted injection in the COApl, but slightly involved the lateralmost COApm (**Figure 4A**). In both cases, the pipette track labeled a few cells in the caudal ABp and AHAl. In addition, cases B0815, B0816, and B0817 were centered in the caudal COApm and case B0880 was centered in the COApl (not shown). In all these cases, labeled fibers arising from the injection site used three different pathways (as defined in the rat by Petrovich et al., 1996) to reach the ventral striatum, namely the *stria terminalis*, the *ansa peduncularis* (running through the interstitial nucleus of the posterior limb of the anterior commissure, IPAC, and substantia innominata, SI) and the longitudinal association bundle (which runs rostral and ventral to reach the Tu, see Johnston, 1923). These pathways gave rise to terminal fields in the midcaudal Acb and Tu.

In the injections centered in the COApm, the AcbC showed labeled fibers in its ventral portion (**Figures 4C–E**). Sparse labeled fibers were present in most of the shell of the Acb, including its rostral tip, whereas dense terminal fields were observed in the periphery of the caudoventral LAcbSh (**Figure 4E**) and in the ventral aspect of the MAcbSh, next to some cell bridges of the ventral striatum (CB, **Figure 4C**; see below). In contrast,

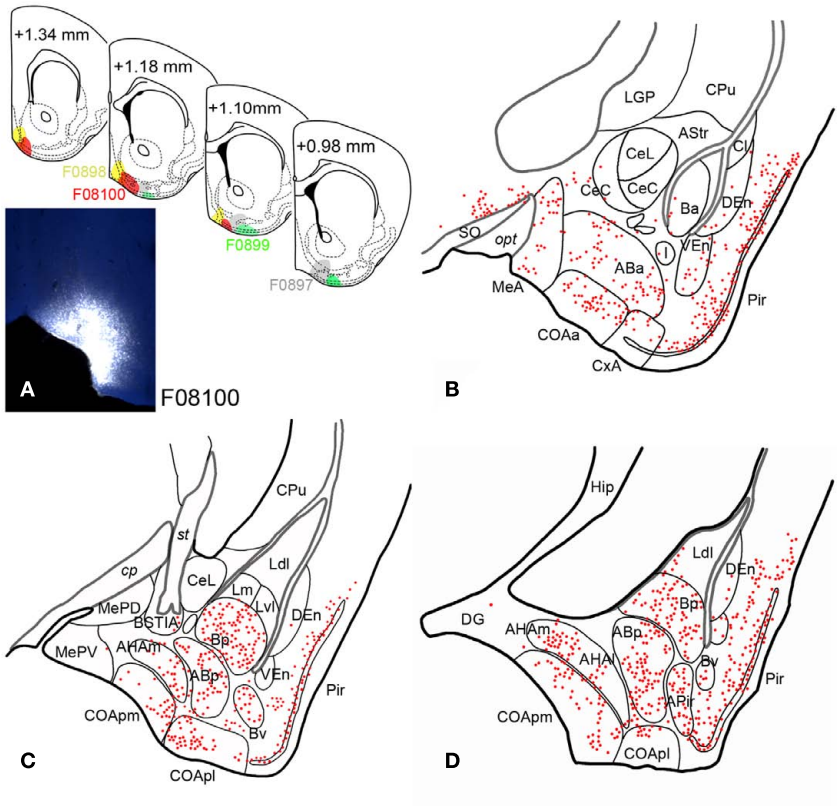

FIGURE 3 | Retrograde labeling in the pallial amygdala after tracer injections in the olfactory tubercle. (A) Semi-schematic drawings of coronal sections through the ventral striatum of the mouse brain showing the extent of fluorogold injections in the Tu, with indication of the antero-posterior coordinate relative to Bregma. The photomicrograph shows the injection site in case F08100, which encompasses the anteromedial island of Calleja. The resulting retrograde labeling is mapped in **(B–D)**. **(B–D)** Camera lucida drawings of frontal sections of the amygdala of a mouse mapping the retrograde labeling observed after an injection of fluorogold in the ventromedial olfactory tubercle (F08100). Note that retrogradely labeled neurons appear both in olfactory and vomeronasal nuclei and also in non-chemosensory amygdaloid structures, such as the basolateral amygdaloid complex.

in injection R0341 (centered in the COApl), the caudal AcbC showed sparse labeled fibers in its medial portion (see pattern in **Figure 9A**) and only a few labeled fibers were present in the AcbSh (**Table 2**).

The injections in COApm and COApl rendered a similar pattern of anterograde labeling in the rest of the ventral striatum, although the labeling resulting from injections in the COApm (e.g., B0415) was always denser than that observed following the injection in the COApl (R0341). After these injections, the densest terminal fields in the ventral striatum were observed in some of the CB (**Figures 4C,D**) and in parts of the caudomedial Tu next to them, where most of the anterograde labeling appeared in layer 3 (inset in **Figure 4D**) in close association with the islands of Calleja dorsal to it (ICj; **Figure 4B** and asterisks in **Figures 4D,E**). Regarding this, a relatively dense terminal field was associated with the lateral aspect of the ICjM (see inset in **Figure 4C**). Therefore, injections involving the caudal cortical amygdala resulted in prominent anterograde labeling in the CB and ICj (including the ICjM, see **Table 3**). Although much less dense, a similar distribution of anterograde labeling was found in the contralateral ventral striatum (**Tables 2–3**), probably connected with a compact bundle of labeled fibers located dorsally in the posterior part of the anterior commissure (*acp*) that appeared after large injections encompassing the COApm/pl.

Injection in the anterior cortical amygdala. Injection B0324 was centered in the caudal aspect of the CxA and the lateral edge of the COAa (**Figure 4A**), but the pipette track also labeled a few cells in the anterior part of the Ba and in the amygdalostriatal transition area (AStr). Labeled fibers arising from the injection site entered the *stria terminalis* to end in the ventral striatum. Moreover, labeled fibers in the *ansa peduncularis* (running through the IPAC) also contributed to the labeling in the LAcbSh and caudal AcbC, whereas labeled fibers that ran through the longitudinal association bundle mainly innervated the olfactory tubercle.

In contrast to the injections in the posterior cortical amygdala, in this case conspicuous anterograde labeling was found throughout the antero-posterior axis of the Acb including its rostral tip (**Table 2**) and even reached the medial anterior olfactory nucleus (not shown). In the AcbSh labeling formed three main

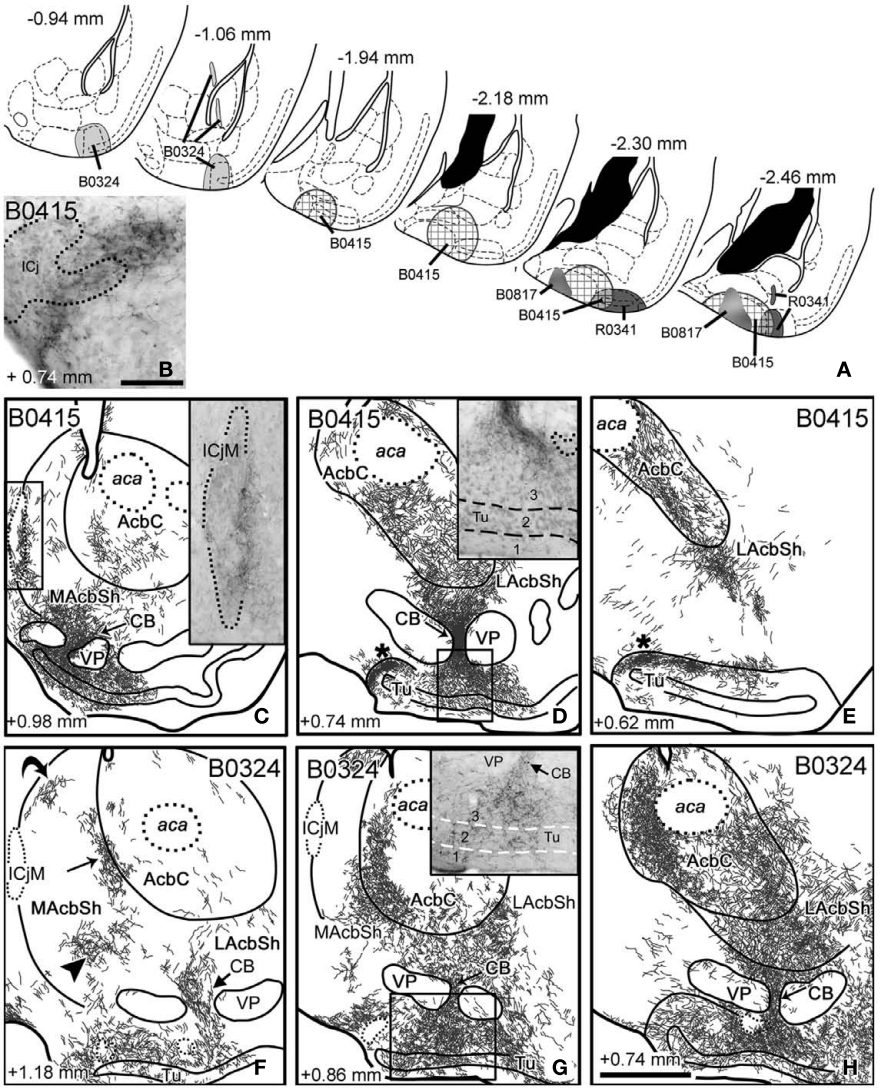

FIGURE 4 | Anterograde labeling in the ventral striatum after tracer injections in the cortical amygdala. (A) Semi-schematic drawings of frontal sections through the amygdala of the mouse showing the extent of the tracer injections in the cortical amygdala indicating the antero-posterior coordinate relative to Bregma. **(B)** High-power microphotograph of a toluidine blue-counterstained section showing the anterograde labeling in the islands of Calleja after an injection of BDA centered in the COApm (B0415). **(C–E)** Anterograde labeling in the ventral striatum resulting from a tracer injection centered in the COApm (B0415). The asterisks in **(D,E)** indicate a labeled terminal field in the caudomedial Tu and adjacent islands of Calleja. Inset in C shows the meshwork of labeled fibers apposed to the medial aspect of the ICjM. Labeling in the CB extends into layer 3 of the Tu [inset in **(D)**]. **(F–H)** Schematic drawings of frontal sections through the ventral striatum of a mouse that received an injection of BDA in the CxA (B0324), showing the resulting anterograde labeling. Three arrows in **(F)** point to the three main terminal fields in the MacbSh, and a fourth arrow remarks the dense innervation of a cell bridge. Labeling in the Tu occupies layers 2 and 3 but also invades the deepest layer 1 [inset in **(G)**]. Arrows in **(G,H)** also point to the innervation of the striatal cell bridges. For abbreviations, see list. Calibration bar in **(B)** = 50 μm. Scale bar in **(H)** = 400 μm [also valid for **(C–G)**].

terminal fields located in the medial (arrowhead and straight arrow in **Figures 4F,G**), ventral (**Figures 4G,H**), and caudolateral shell (**Figure 4H**). In addition, a small group of labeled fibers occupied the boundary between the MAcbSh and the rostral lateral septum (curved arrow in **Figure 4F**). At mid-rostral levels, the dense terminal fields that occupied the ventral portion of the MAcbSh and LAcbSh seemed to be continuous, through the CB, with labeling in the whole mediolateral extension of the Tu. In this injection, anterograde labeling in the Tu was dense in all three layers (maybe slightly denser in layer 3; see inset in **Figure 4G**), but showed no evident association with the ICj (see **Table 3**).

In the caudal AcbC we observed a dense terminal field that extended ventromedially in the rostral direction, innervating the boundary with the MAcbSh (**Figures 4G,H**). In contrast, the ventrolateral AcbC showed less dense anterograde labeling, which appeared continuous with the terminal field found in the LAcbSh (**Figure 4H**).

Table 2 | Semiquantitative rating of the density of the anterograde labeling found in three rostro-caudal levels of the nucleus accumbens shell and core (columns) after different injections in the cortical and deep pallial amygdala (rows).

	MAcbSh			LAcbSh			AcbC		
	r (from +1.78 to +1.54 mm)	i (from +1.42 to +1.18 mm)	c (from +1.10 to +0.86 mm)	r (from +1.34 to +1.18 mm)	i (from +1.10 to +0.98 mm)	c (from +0.86 to +0.74 mm)	r (from +1.94 to +1.70 mm)	i (from +1.54 to +1.34 mm)	c (from +1.18 to +0.98 mm)
CORTICAL AMYGDALA									
R0341 COApl	–	/	/	–	/	X	–	/	X
from −2.30 to −2.46 mm			b			b			b
B0415 COApm + COApl	–	/	/	–	/	XX	–	/	X
from −1.94 to −2.46 mm		b	b		b	b		b	b
B0817 COApm	/	XX	X	–	X	/	–	/	–
from −2.46 to −2.80 mm		b	b		b				
B0324 CxA (+ COAa)	X	XX	XX	X	XX	XX	X	X	XX
from −0.94 to −1.06 mm		B	b			b	b	b	B
DEEP PALLIAL AMYGDALA									
B0310 Ba	XXXX	XXX	XX	XXX	XXX	XXX	XXXX	XXX	XXX
from −1.06 to −1.82 mm		b	b	B	B	B	B	b	b
R0336 Bp	X	XXX	XXX	/	X	XX	XX	XXX	XXXX
from −2.30 to −2.70 mm		b	B			b		B	B
B0311 ABa	/	X	XX	/	/	X	/	/	X
from −0.58 to −0.82 mm			b		b	B		B	B
R0324 ABp	X	XX	XX	X	X	XX	XX	XX	XX
−1.82 mm			b	b	B	B	b		
R0335 ABp		XXX	XXX	XX	XX	XXX	XXX	XXX	XXX
−2.18 mm		B	B	b	B	B	B	B	B
R0311 AHAl	/	X	XX	/	X	X	/	X	XX
from −1.82 to −1.94 mm		b	B			B		b	B
R0305 Lvl	XX	XX	X	XX	XXX	XXX	XXX	XXX	XXX
−1. 82 mm	B	B	B	B	B	B	B	B	B
R0330 Lvl (Ldl + CPu)	XX	XX	XXX	X	XX	XX	XXX	XXX	XXX
−1.70 mm	B	B	B	B	B	B	B	B	B
B0334	X	X	XX	/	X	X	X	XX	XXX
Lvl(+Ldl + Lm + AStr)			b			b		b	b
from −1.70 to −2.30 mm									

The rostro-caudal extent (coordinates from Bregma) of each injection is indicated. The relative density is indicated as follows: –, no labeling; /, very few fibers; X, few fibers; XX moderate density; XXX dense terminal field; XXXX very dense terminal field; XXXXX extremely dense terminal field; B, conspicuous contralateral labeling; b, scarce contralateral labeling. For abbreviations, see list.

In this case, labeling in the Acb, Tu, and CB was bilateral with clear ipsilateral dominance (**Tables 2** and **3**, more evident in the MAcbSh and caudal AcbC, see **Table 2**). Labeled fibers were seen to cross the midline through the *acp* but did not conform conspicuous bundles.

Anterograde labeling in the deep pallial amygdala after injections in the cortical amygdala

To check whether the associative nuclei of the deep pallial amygdala (L, B, and AB) can indirectly relay chemosensory information to the ventral striatum, we studied the intra-amygdaloid projections from the cortical (chemosensory) amygdaloid nuclei to the deep pallial amygdala. Injections in the vomeronasal-recipient COApm gave rise to anterograde labeling in the AB (**Figure 5A**), particularly dense in the posterior part of this nucleus, with sparse fibers observed in the B and L. In contrast, injections in the olfactory-recipient nuclei COApl rendered moderate-to-dense anterograde labeling in the B, mainly in its lateral part, extending into the ventrolateral L (**Figure 5B**). Finally, the injection placed in the CxA (which receives olfactory projections, but also a minor vomeronasal input, Gutiérrez-Castellanos et al., 2010), resulted in abundant anterograde labeling in both the AB and B, which was especially dense in their lateral aspect (**Figure 5C**). In this case, moderately dense anterograde labeling was also observed in the Lvl (**Figure 5C**).

Anterograde labeling in the ventral striatum after injections in the deep pallial amygdala

Ten injections were aimed at the deep pallial amygdala (**Tables 2** and **3**; **Figures 6–8**): three of them were confined to the B, three were located in the AB, one in the AHAl and the last three injections were restricted to the L.

Table 3 | Semiquantitative rating of the density of the anterograde labeling found in three rostro-caudal levels of the olfactory tubercle (Tu; the antero-posterior coordinates to Bregma are indicated), the cell bridges of the ventral striatum (CB), and in association with the islands of Calleja (ICj) and the major island of Calleja (ICjM) (columns), after different injections in the cortical and deep pallial amygdala (rows).

	Tu			CB	ICj	ICjM
	r (from + 1.98 to + 1.42 mm)	i (from + 1.34 to + 0.74 mm)	c (from + 0.62 to + 0.02 mm)			
CORTICAL AMYGDALA						
R0341 COApl	/	X	XX	XX	XX	X
from −2.30 to −2.46 mm		b	b	b		
B0415 COApm + COApl	X	XX	XXX	XXX	XXX	XXX
from −1.94 to −2.46 mm		B	b	B	B	B
B0817 COApm	XX	XXX	/	XXX	XXX	XXX
from −2.46 to −2.80 mm						b
B0324 CxA (+ COAa)	XX	XX	XXX	XXX	/	/
from −0.94 to −1.06 mm		b	b	b		
B0310 Ba	XXXXX	XXXX	XXX	XXXX	X	/
from −1.06 to −1.82 mm	B	B	B	B	B	
R0336 Bp	XX	XXX	XX	XXX	X	X
from −2.30 to −2.70 mm	b	B	B	B	b	b
DEEP PALLIAL AMYGDALA						
B0311 ABa	X	X	X	XX	X	X
from −0.58 to −0.82 mm	b	b	b	b	b	b
R0324 ABp	XX	XX	XX	XX	/	–
−1.82 mm	B	B	B	B	b	
R0335 ABp	XXX	XXX	XXX	XXX	X	/
−2.18 mm	B	B	B	B	b	b
R0311 AHAl	X	XX	XX	X	XX	XX
from −1.82 to −1.94 mm	b	B	B	B	b	B
R0305 Lvl	XXX	XXX	XXX	XXX	X	/
−1. 82 mm	B	B	B	B	B	
R0330 Lvl (Ldl + CPu)	XXX	XX	XX	XXX	X	/
−1.70 mm	B	B	B	B	B	
B0334 Lvl(+Ldl + Lm + AStr)	/	X	X	X	/	/
from −1.70 to −2.30 mm						

The rostro-caudal extent (coordinates from Bregma) of each injection is indicated. The density of labeling is scored according to the following code: –, no labeling; /, very few fibers; X, few fibers; XX, moderate density; XXX, dense terminal field; XXXX, very dense terminal field; XXXXX, extremely dense terminal field; B, conspicuous contralateral labeling; b, scarce contralateral labeling. For abbreviations, see list.

Injections in the basal nucleus. Injection B0310 was restricted to the medial aspect of the Ba, although a few cells in the anterior edge of the AStr were apparently labeled by the pipette track (**Figure 6A**). A bundle of thick, labeled fibers entered the *stria terminalis*, where they could be followed up to the Acb. A different group of labeled fibers ran in the *ansa peduncularis* (through the IPAC and SI) and seemed to be continuous with the labeling in the caudal LAcbSh. Moreover, labeled fibers left the injection site and run rostralwards (through the longitudinal association bundle) to innervate the LOT and, after crossing the ventral anterior amygdala (AAV) gave rise to a dense terminal field in the Tu (**Figures 6B,C**).

The Acb displayed dense fields of anterograde labeling in all its divisions (**Table 2**). In its lateral half, labeling was very dense and showed a complex patchy distribution (**Figure 6C**), whereas in the medial AcbC labeling was mainly composed of sparse labeled fibers except for dense terminal field in its rostral aspect (**Figure 6B**). The MAcbSh displayed patchy, dense fiber labeling mainly confined to its ventral aspect (**Figures 6B,C**). This labeling showed continuity (through the CB, **Figure 6C**) with even denser terminal fields in the medial Tu (**Figures 6B,C**). In contrast, in the dorsal aspect of the MAcbSh only sparse labeled fibers were visible that did not make up well-defined terminal fields (**Figures 6B,C**). The LAcbSh showed a dense terminal field that was also continuous with the extremely dense labeling found in the lateral CB and Tu (**Figure 6C**). In the Tu, the labeling was dense in layer 3 and very dense in layer 2 (**Figures 6B,C** and inset in **Figure 6C**), but showed no clear association with the deep ICj or ICjM. On the contrary, the anterograde labeling in the Tu showed a gap where a superficial ICj was present (**Figure 6C** and inset). However, a few, thick, labeled fibers always reached these superficial ICj (see inset in **Figure 6C**).

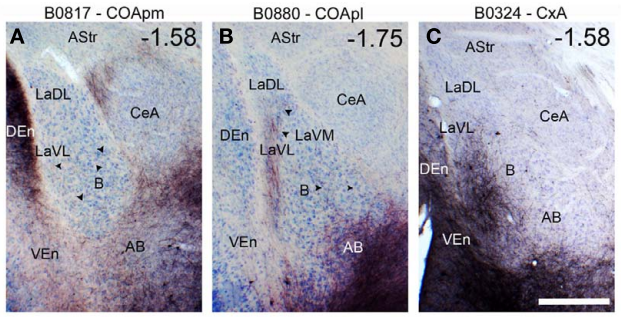

FIGURE 5 | Anterograde labeling in the multimodal amygdaloid nuclei following tracer injections in the chemosensory amygdala. (A) Dense anterograde labeling observed in the accessory basal nucleus of the amygdala following a BDA injection in the COApm, which is the main cortical target of vomeronasal information relayed by the AOB. A few scattered fibers are also present in the basal nucleus of the amygdala (arrowheads). **(B)** Anterograde labeling found in the basolateral complex of the amygdala after a BDA injection in the COApl. Note the band of labeled fibers in the lateral aspect of the B and the ventrolateral L. In addition, scattered fibers are observed throughout the B. **(C)** Anterograde labeling in the basolateral amygdaloid complex following a BDA injection centered in the CxA, which also affected a small portion of the neighboring COAa. Thre resulting anterograde labeling is especially dense in the lateral part of the B and AB, and extends into the ventrolateral L. For abbreviations, see list. Scale bar in **(C)** = 500 μm, valid for the whole figure. The antero-posterior coordinate relative to Bregma is indicated in the upper right corner of each photograph.

In this injection in the Ba, labeled fibers were seen to cross the midline through the *acp*. Dealing with this, the contralateral Acb (especially the LAcbSh and rostral AcbC, **Table 2**) and the rest of the contralateral ventral striatum (**Table 3**) showed a low density of labeled fibers.

Two injections (B0336 and R0336) were located in the Bp. Injection B0336 encompassed the caudolateral Bp, whereas R0336 was a restricted to the caudal portion of the Bp (**Figure 6A**). Although labeled fibers connecting the injection site with the ventral striatum were similar to those found in the previous case, the pattern of anterograde labeling in the ventral striatum differed substantially from that found after injections in the Ba. Thus, the caudomedial AcbC showed extremely dense anterograde labeling (**Figure 6E**) that was apparently connected with a dense terminal field in the bed nucleus of the *stria* terminalis (BST, not shown). Labeling also extended into the MAcbSh where it was very dense (**Figures 6D,E**), with patchy distribution (arrowheads, **Figure 6E**). A few labeled fibers in the periphery of the AcbSh seemed to enter the ICjM (**Figure 6E**). Labeling in the periphery of the MAcbSh could be followed through the medial CB into the medialmost Tu (**Figure 6E**), where labeled fibers were found in deep layer 1 and in layers 2 and 3 (inset in **Figure 6E**). Only a few labeled fibers entered the medial ICj (see inset in **Figure 6E**). In the LAcbSh anterograde labeling was diffuse and its density gradually decreased from caudal to rostral (**Table 2**; **Figures 6D,E**). In these injections, labeled fibers crossed the midline trough the *acp* and gave rise to scattered but conspicuous anterograde labeling in the contralateral ventral striatum (**Tables 2** and **3**).

Injections in the accessory basal nucleus. Injection B0311 was centered in the rostral tip of ABa, and also affected the deepest aspect of the COAa and the intercalated cell masses of the amygdala (I), as well as a few cells in the AAD and the SI (**Figure 7**). In contrast to injections in B, this case displayed scarce labeling in the Acb and the Tu (**Table 2**; **Figure 7B**). Three groups of fibers could be tracked from the injection to the ventral striatum. First, thick, labeled fibers ran through the *stria terminalis* up to terminal fields in the BST and dorsolateral, caudal AcbC (not shown). Some labeled fibers followed the *ansa peduncularis* (through the IPAC) to the caudalmost LacbSh and the ventral pallidum (**Figure 7B**). Finally, fibers in the longitudinal association bundle gave rise to a dense terminal meshwork in the horizontal limb of the diagonal band nucleus (HDB) that extended into the medialmost CB (inset in **Figure 7B**) and the medial Tu, where it innervated all three layers. A few labeled fibers apparently entered some ICj (inset in **Figure 7B**), and surrounded the ICjM (**Figure 7B**). Moreover, the ventral MAcbSh displayed scarce fiber labeling apparently connected with the bundles innervating the HDB and/or VP (**Figure 7B**). The contralateral, caudal ventral striatum also showed few labeled fibers (see **Tables 2** and **3**), which were observed to cross the midline through the *acp*.

Two small injections (R0324 and R0335) located in the ABp (with a few labeled cells in the AHAl in case R0335; **Figure 7A**) revealed a pattern of fiber labeling in the ventral striatum substantially more extensive than the one observed following the injection in the ABa (compare the **Figures 7B–D**). The amygdalofugal fibers followed the three pathways described above. First, thin labeled fibers of the *stria terminalis* apparently gave rise to a moderately dense terminal field in the whole AcbC and the ventral MAcbSh (**Figures 7C,D**). Second, labeled fibers in the *ansa peduncularis* gave rise to a terminal field extending from the IPAC to the caudal LAcbSh, where labeling was less dense (**Table 2**; **Figures 7C,D**). Finally, labeled fibers in the longitudinal association bundle reached the Tu, where they preferentially innervated layers 2, 3, and 1b of its central aspect (inset in **Figure 7D**). Labeling in the Tu was continuous, through the CB, with the one observed in the ventral AcbSh (see arrows in **Figures 7C,D**). Few labeled fibers were associated to the outer edge of most of the ICj (inset in **Figure 7C**) and, to a lesser extent, to the inner margin of the ICjM (arrowhead in **Figure 7C**). In both injections, the contralateral ventral striatum also showed a moderate density of anterograde labeling (**Tables 2** and **3**).

Injection in the amygdalohippocampal area. A small injection (R0311) was restricted to the rostral tip of the AHAl (**Figure 7A**). Labeled fibers in the *stria terminalis* apparently innervated the AcbC (where labeling decreased from caudal to rostral, see **Table 2**), especially its ventral half (**Figures 7E,F**) and the midcaudal MAcbSh, where labeled fibers were preferentially found in the medial edge of the nucleus (arrow in **Figure 7F**) and next to the core-shell boundary (**Figures 7E,F**). A dense terminal field was closely associated to the inner ICjM (see inset in **Figure 7F**). The labeled bundles in the IPAC/SI could be followed rostrally up to the midcaudal LAcbSh, where sparse anterograde labeling was observed (**Figure 7F**). Finally, labeled fibers running in

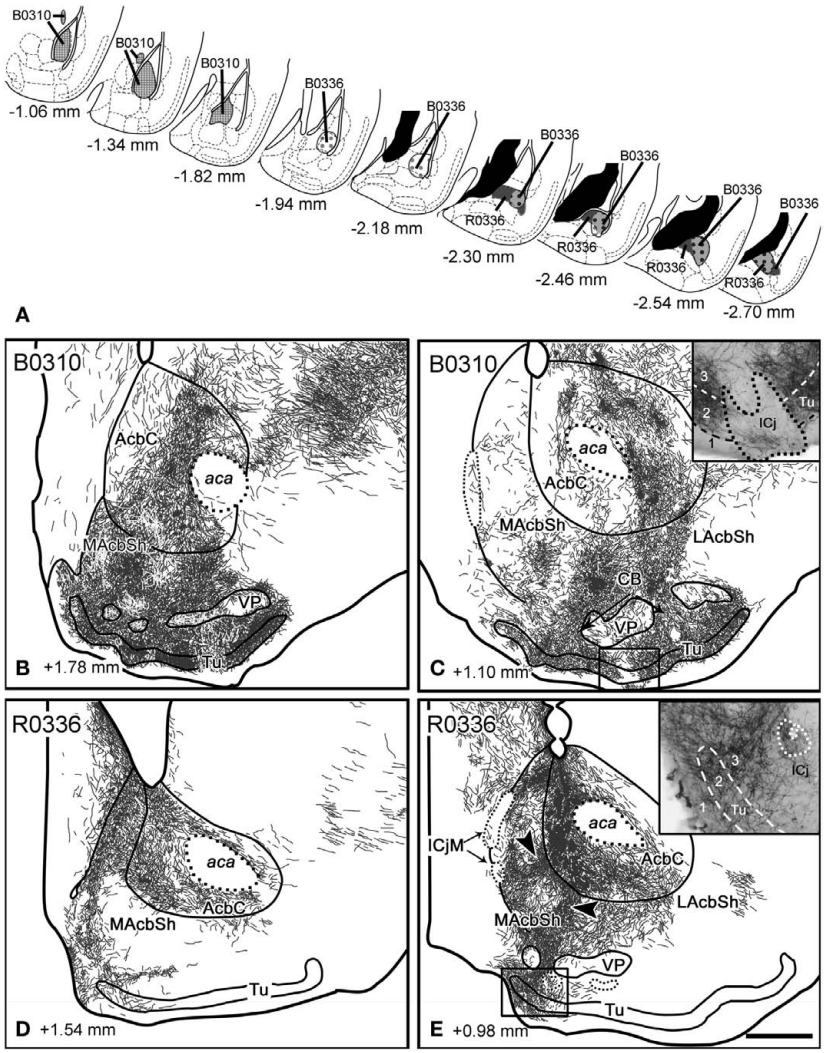

FIGURE 6 | Anterograde labeling in the ventral striatum after tracer injections in the basal nucleus of the amygdala. (A) Semi-schematic drawings of frontal sections showing the extent of the tracer injections in the basal nucleus of the amygdala, with indication of the antero-posterior coordinate relative to Bregma. **(B,C)** Anterograde labeling found in the ventral striatum after a tracer injection in the Ba (B0310). Although the ICj are nearly devoid of labeling, a few thick, labeled fibers enter the clusters of granule cells [see inset in **(C)**]. Labeling in the AcbSh shows continuity with the one in the Tu through the CB. Labeling in the Tu occupies layers 2 and 3, whereas layer 1 is virtually free of labeling [inset in **(C)**]. **(D,E)** Anterograde labeling in the ventral striatum after injection R0336, which involved a large portion of the Bp. Labeling in the core of the Acb apparently shows continuity with the one in MAcbSh [see arrowheads in **(E)**] and, through it, with the labeling in the CB and medial Tu. labeling in the Tu occupies not only layers 2 and 3 but also deep layer 1 [inset in **(E)**]. For abbreviations, see list. Scale bar in **(E)** = 400 μm, valid for the whole figure.

the longitudinal association bundle innervated the HDB and all three layers of Tu, preferentially in its medial half (**Figure 7F**). This terminal field, which was connected with the one in the AcbSh through the CB (see asterisk in **Figures 7E,F**), also included dense labeled fibers in close association with the medial ICj (**Figure 7F**).

Labeled fibers crossed the midline trough the *acp* to innervated some structures of the contralateral, caudal ventral striatum (**Tables 2** and **3**).

Injections in the lateral nucleus. Three injections were aimed at the L (see **Figure 8**). Injection R0330 was centered in the rostral Lvl, although it also encompassed the ventral part of the Ldl and involved a few cells in the caudoventral CPu. Injection R0305 consisted of a small injection restricted to the Lvl at intermediate antero-posterior levels. Finally, a large BDA injection encompassed the whole caudal L (Ldl, Lvl, and Lm) and the AStr (B0334). In these three injections, labeled fibers ran in the *stria terminalis* up to the AcbC, where they gave rise to the densest terminal field in the ventral striatum, which extended to the adjacent, ventralmost CPu (**Table 2**; **Figures 8B–E**). From the AcbC, anterogradely labeled fibers extended to the ventral AcbSh, where they formed a conspicuous terminal field (**Figures 8B–D**), whereas the dorsal MAcbSh (interposed between the core and the medial

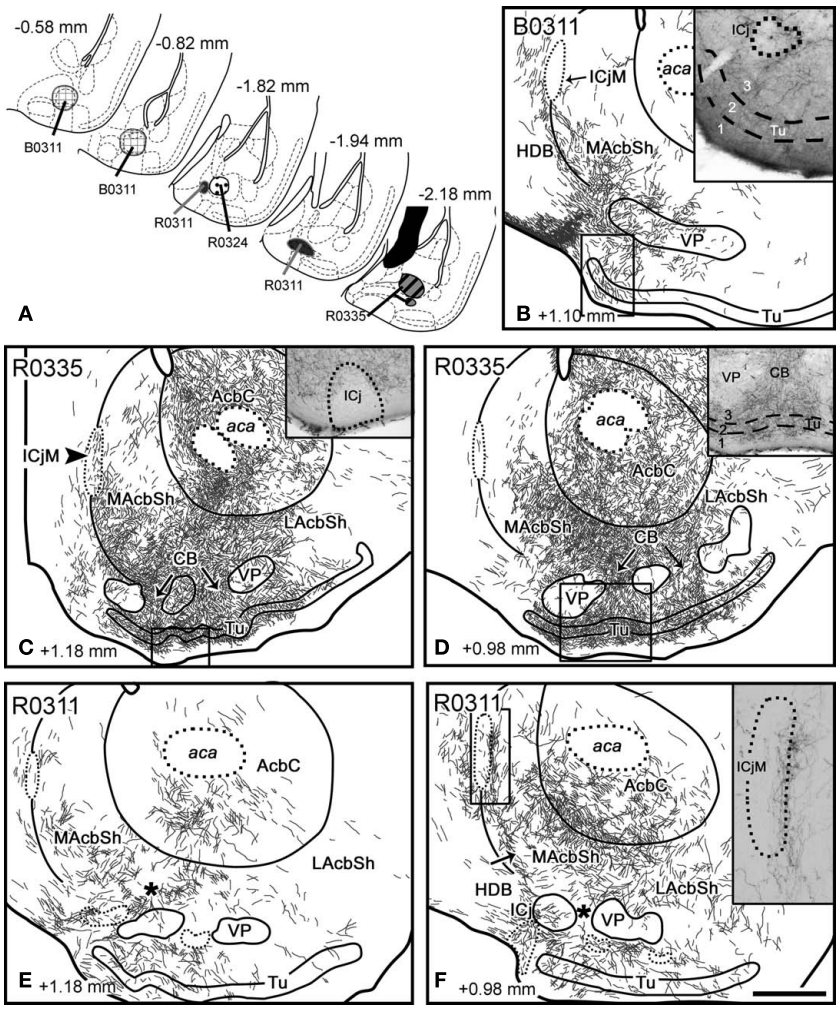

FIGURE 7 | Anterograde transport in the ventral striatum after tracer injections in the accessory basal amygdaloid nucleus and amygdalohippocampal area. (A) Semi-schematic drawings of frontal sections showing the extent of the tracer injections in the accessory basal nucleus of the amygdala. The antero-posterior coordinate relative to Bregma is indicated in each section. **(B)** Anterograde transport in the MAcbSh and medialmost caudal Tu after a tracer injection in the ABa (B0311). Scattered labeled fibers are present in the ICj and in all three layers of the Tu (inset). **(C,D)** Frontal sections through the ventral striatum of a mouse that received an RDA injection in the ABp(R0335; no counterstaining). Besides extensive labeling in the Acb core and shell (especially in the LAcbSh), a labeled terminal field is found next to some of the ICj [inset in **(C)**] and in the ICjM [arrowhead in **(C)**]. In the Tu, anterograde labeling is found in layers 2 and 3 and in deep layer 1 [inset in **(D)**]. **(E,F)** Anterograde labeling in the ventral striatum after an RDA injection restricted to the lateral AHA (R0311) (no counterstaining). Moderately dense labeling occupies the ventral core as well as parts of the medial and lateral shell of the Acb. Scattered labeled fibers are also found in the neighboring CB (asterisks) and in the Tu. In addition, conspicuous terminal fields are found in the medial ICj and, especially, next to the ICjM [see inset in **(F)**]. For abbreviations, see list. Scale bar in **(F)** = 400 μm, valid for the whole figure.

septum), was virtually devoid of labeling (**Figures 8B–D**). Labeling in the ventral AcbSh was continuous, through the CB, with labeling in the Tu (**Figures 8C–E**). Anterogradely labeled fibers displayed a clear association with the most medial ICj (see inset in **Figure 8D**), but not with the ICjM (see **Figure 8D**). After the small injections in the rostral L (R0305, R0330), labeling in the Tu was particularly dense, and preferentially occupied layer 3 and (to a lesser extent) layer 2 (**Figures 8B–D** and inset in **Figure 8B**).

In addition, some labeled fibers ran through the *ansa peduncularis* (through the SI and the IPAC) and gave rise to a moderate-to-dense terminal field in the midcaudal LAcbSh (**Figure 8E**). Finally, a small number of labeled fibers were seen in longitudinal association bundle, apparently giving rise to anterograde labeling in the Tu.

In all the injections encompassing the L, anterograde labeling in the ventral striatum was bilateral with ipsilateral dominance (see **Tables 2** and **3**).

DISCUSSION

Our work combines anterograde and retrograde tracing to analyze the projections of the amygdala to the ventral striatum, with emphasis on the putative pathways allowing the transfer of chemosensory information to the reward system of the brain.

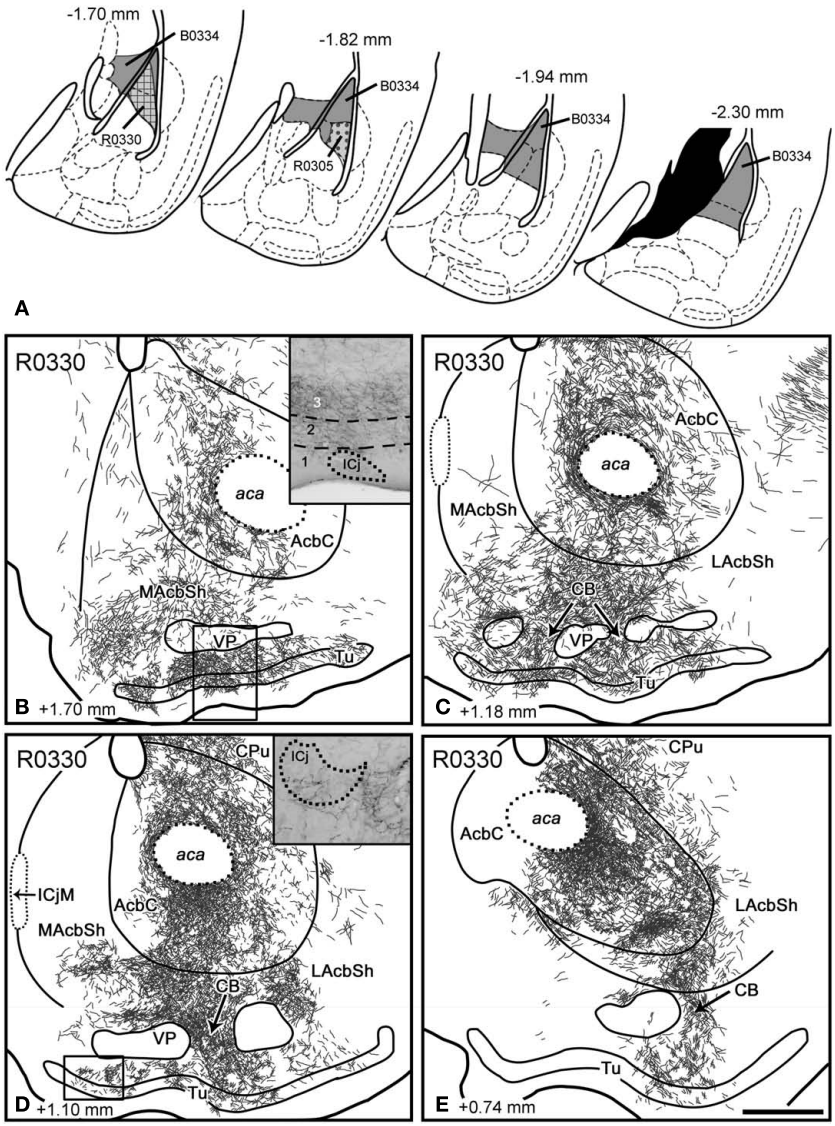

FIGURE 8 | Anterograde labeling in the ventral striatum after tracer injections in the lateral nucleus of the amygdala. (A) Semi-schematic drawings of frontal sections through the amygdala depicting the extent of tracer injections in the lateral nucleus. The antero-posterior coordinate relative to Bregma is indicated in each section. **(B–E)** Semi-schematic drawings of four frontal sections through the brain of a mouse that received an RDA injection in the Lvl and Ldl (R0330), showing the distribution of anterograde labeling in the ventral striatum. Labeling occupies parts of the core and shell of the Acb, a large portion of the Tu [layers 2 and 3, inset in **(B)**] and those CB linking both structures (arrows). In some islands of Calleja a few, thick, labeled fibers are seen in the clusters of granule cells [inset in **(D)**]. For abbreviations, see list. Scale bar in **(E)** = 400 μm, valid for the whole figure.

To properly interpret our results we should first discuss some limitations of the tract-tracing techniques we have used.

METHODOLOGICAL CONSIDERATIONS

In the first part of the study we have used the retrograde transport of fluorogold and biotin- and rhodamine-labeled dextran amines to label the amygdaloid afferents to the ventral striatum. Although dextran amines are generally used as anterograde tracers, in certain conditions they also reliably render retrograde transport (Rajakumar et al., 1993; Reiner et al., 2000; Schofield, 2008) and they have been used as such in mammals (Schofield and Cant, 1996). In fact, our retrograde tracing experiments replicate the results of similar experiments in rats using fluorogold (Brog et al., 1993). In addition, our results of retrograde tracing of the amygdalo-striatal pathways are consistent with those of anterograde tracing of the same projections (see below).

In the second part of the study, we have injected dextran amines in the amygdala to analyze the anterograde transport to the ventral striatum and within the amygdala itself. Since in our experimental conditions dextran amines are transported both retrogradely and anterogradely, in the interpretation of the results we take into account the possibility of fiber labeling due to axon collaterals from retrogradely labeled cells. In addition, in every injection anterogradely labeled fibers can be tracked through previously defined

tracts (see below) from the injection site to the terminal fields in the ventral striatum. This indicates that the bulk of the labeling found in the striatum originates in cells located in the injection site in the amygdala. On the other hand, the projections revealed by anterograde labeling in the amygdala have been confirmed by means of retrograde labeling from injections in the striatum, except for a single case, the projection from the lateral nucleus of the amygdala to the olfactory tubercle, as discussed below.

DIRECT AND INDIRECT PATHWAYS THROUGH THE AMYGDALA RELAY CHEMOSENSORY INFORMATION TO THE VENTRAL STRIATUM

Our results demonstrate that both cortical and deep amygdaloid nuclei extensively innervate the ventral striatum. Given that the cortical amygdaloid nuclei (COAa, CxA, COApl, and COApm) receive olfactory and vomeronasal projections from the olfactory bulbs, it is likely that the amygdalo-striatal projections originated in these nuclei convey chemosensory information. In addition, our results show that intra-amygdaloid projections originated from these cortical amygdaloid nuclei innervate the lateral, basal, and accessory basal nuclei of the basolateral complex, which are considered associative nuclei (they receive important projections from unimodal and multimodal areas from the thalamus and cortex, see Turner and Herkenham, 1991; McDonald, 1998; Swanson and Petrovich, 1998). These projections from the chemosensory cortical amygdala to the deep associative nuclei are consistent with previous data reported in rats. The projection from the vomeronasal-recipient COApm to the AB was observed by Canteras et al. (1992) and Kemppainen et al. (2002). Regarding the COApl, it is included as part of the periamygdaloid cortex by several authors (see Pitkänen, 2000), and a number of studies show projections from the periamygdaloid cortex to the L (Ottersen, 1982; Luskin and Price, 1983; Majak and Pitkänen, 2003) and to the B (Ottersen, 1982; Luskin and Price, 1983). Finally, to our knowledge the connections of the CxA have not been previously analyzed, but a previous study using the retrograde transport of HRP in the rat showed retrogradely labeled cells in this area following injections in the L and B (Ottersen, 1982; see his Figures 2D and 5F). None of these intra-amygdaloid projections had been previously shown in mice. Therefore, both the direct projections from the chemosensory cortical amygdala and the indirect projections from the associative amygdaloid nuclei may convey chemosensory information to the ventral striatum.

ORGANIZATION OF AMYGDALO-STRIATAL PATHWAYS IN THE MOUSE

These amygdalo-striatal projections course through three pathways, namely the *stria terminalis*, the *ansa peduncularis*, and the longitudinal association bundle, in agreement with previous descriptions (Johnston, 1923; Kelley et al., 1982; Petrovich et al., 1996). In general, the amygdaloid fibers terminating in the AcbC and dorsomedial AcbSh course through the *stria terminalis* and represent a rostral extension of the terminal fields in the BST. A second amygdalo-striatal pathway courses through the *ansa peduncularis* crossing the SI/IPAC and entering the lateral AcbSh, and maybe the caudolateral AcbC. A third contingent of amygdalo-striatal fibers runs rostralwards through the longitudinal association bundle (Johnston, 1923) thus reaching directly the caudal Tu and adjacent structures. Fibers running in all three pathways might contribute to the innervation of the ventral aspect of the AcbSh and the adjoining CB.

The termination fields of the main amygdaloid projections to the ventral striatum are summarized in **Figure 9**. As it can be observed, virtually all the divisions of the ventral striatum receive inputs from one or several amygdaloid nuclei, thus depicting a complex pattern of amygdalo-striatal projections.

Ventral striatal projections of the cortical amygdaloid nuclei

Our experiments reveal important amygdalo-striatal projections arising from several cortical amygdaloid nuclei which, according to the present results, were probably underestimated in previous studies. The anterior aspect of the cortical amygdala displays substantial projections to the Acb and Tu/CB apparently originated from deep cells in the CxA/COAa boundary (**Figures 2B** and **3B**). This projection was also suggested by previous observations in rats (McDonald, 1991b) and monkeys (Friedman et al., 2002). Regarding the posterior cortical amygdala, our results show that a number of deep cells of the COApm and COApl are retrogradely labeled by injections in the Tu. These projections are confirmed by the anterograde labeling following injections in the COApm and COApl, which reveal a conspicuous projection to the deep Tu, CB, and some ICj (see below; Úbeda-Bañón et al., 2008), as well as sparse projections to the caudal AcbC and AcbLSh (see **Figure 9**), in agreement with previous results in rats (Canteras et al., 1992).

Our injections in the core and lateral shell of the Acb, also showed retrogradely labeled cells in the LOT. The location of these labeled cells depended on the injection site: whereas tracer injections in the LAcbSh rendered retrograde labeling in layers 2 and 3 of the LOT, those in the AcbC only showed labeled cells in layer 3. These data fully fit the results of anterograde tracing in the rat reported by Santiago and Shammah-Lagnado (2004).

Finally, in agreement with the findings by Brog et al. (1993) in the rat, our results of retrograde labeling demonstrate the presence of important projections to the MAcbSh and Tu arising from the APir. Although we have not performed tracer injections in the APir, experiments of anterograde transport carried out in the rat by Shammah-Lagnado and Santiago (1999) confirm this projection. As suggested previously (Luskin and Price, 1983), these projections might be association fibers, originating from pyramidal cells located in layers II and II.

Ventral striatal projections of the deep nuclei of the pallial amygdala

This pattern of amygdalo-striatal projections originated by the deep pallial amygdala displays three main similarities with the results of previous studies in other mammalian species.

Firstly, as described in rats and cats (Krettek and Price, 1978; Groenewegen et al., 1980; Kelley et al., 1982; Russchen and Price, 1984; McDonald, 1991a,b; Brog et al., 1993; Wright et al., 1996) and in monkeys (Russchen et al., 1985; Price et al., 1987; Friedman et al., 2002; Fudge et al., 2002, 2004), the bulk of the amygdalo-Acb projections arises from deep pallial nuclei (B and AB). Secondly, our results indicate that in mice, like in rats and cats (Krettek and Price, 1978; Wright et al., 1996) the projections from the anterior and posterior parts of the B to the Acb display a rough topography according to which the Ba projects mostly to the anterior

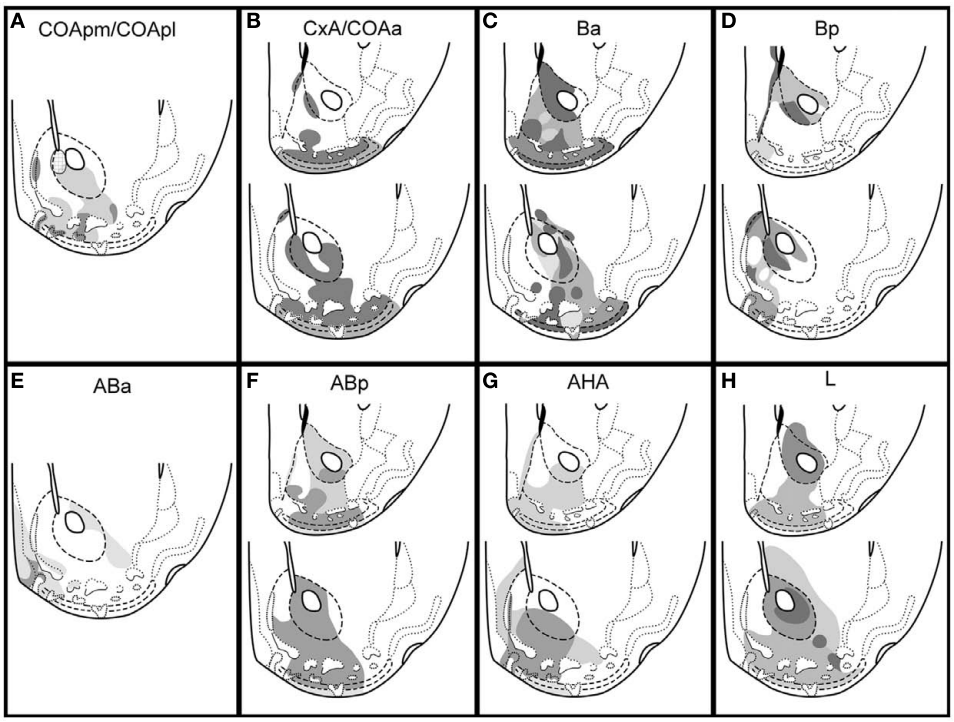

FIGURE 9 | Summary of the projections from pallial amygdala to the ventral striatum in the mouse. Schematic drawings of frontal sections through the ventral striatum of the mouse (rostral on top, caudal bottom), showing the main terminal fields of the projections from the cortical **(A,B)** and deep pallial amygdala **(C–H)** in the ventral striatum. The relative density of the terminal fields, as inferred from our injections, is represented as different gray levels (the darker the denser). The patterned area in the medial AcbC in **(A)** indicates a terminal field that is labeled after the injection in the COApm but not in the injection centered in the COApl. For abbreviations, see list.

and posterolateral Acb/Tu, whereas the Bp projects mainly to the medial posterior Acb/Tu (**Figures 9C,D**). And finally, anterograde transport after injections in B and AB reveal a patchy distribution of labeled fibers in the medial AcbSh (see **Figures 6C,E** and **7B,D**) that recalls the one described in the rat and cat by Krettek and Price (1978). Whether or not these patchy projections are related to inhomogeneities in calbindin-immunoreactivity as reported in the rat (Wright et al., 1996), the similarities in the amygdalo-Acb projections between mice and other mammals are noticeable. This similarity also makes very unlikely that the labeled fibers observed in our material be due to labeling of axonic collaterals from retrogradely labeled cells.

An additional conclusion drawn from our findings is that the AHA and L substantially contribute to the projections from the deep pallial amygdala to the Acb and Tu. Experiments in rats have also demonstrated substantial anterograde transport to the caudal Acb after tracer injections in the AHA (Canteras et al., 1992, posterior amygdala using their nomenclature) and dense retrograde labeling in the AHA following injections in the MAcbSh (McDonald, 1991b; Brog et al., 1993).

Finally, our results clearly indicate that the L, a nucleus usually viewed as the sensory interface of the amygdala (at least in the context of fear conditioning, LeDoux et al., 1990; Pitkänen et al., 1997), shows important projections to the ventral striatum. The existence of this connection has been previously suggested in rats (Kelley et al., 1982; McDonald, 1991b; Brog et al., 1993) and primates (Friedman et al., 2002; Fudge et al., 2002). Our results indicate that these projections mainly arise from the dorsolateral (Ldl) and ventrolateral subnuclei (Lvl, see **Table 1**). This is confirmed by anterograde transport after injections in the L (involving the Lvl and/or Ldl), which display labeled fibers in the midcaudal AcbC (from where they extend into the rostromedial CPu), as well as in the ventral aspect of the MAcbSh and in the LAcbSh (**Figure 9H**). This projection apparently extends into the Tu/CB complex and the ICj, although we could not confirm this observation with retrograde labeling.

Amygdaloid projections to the islands of Calleja and associated territories of the olfactory tubercle

Our tracing experiments reveal not only important amygdaloid projections to the Tu, but also very important connections with other structures including ICj and the CB (see **Figure 9**). The ICj are densely packed groups of small cells that occupy diverse positions within the ventral striatum. Most of them are placed within the Tu, where they are located in layers 2–3 and even impinge upon layer 1 reaching the pial surface. In contrast, the ICjM separates the medial AcbSh from the ventral aspect of the lateral septum. The COApm/COApl and AHA display strong projections to the medial ICjs and ICjM (see **Table 3**). In contrast, the remaining amygdaloid nuclei give rise to limited projections to the ICj, which are relatively rare in the case of the ICjM (see **Table 3**). These results partially agree with previous studies on

the ICj connections indicating that the bulk of the amygdaloid projections to the ICj arose from the cortical nuclei (Krettek and Price, 1978; Fallon, 1983). Recent reports have also described in some detail these projections in rats and mice (Úbeda-Bañón et al., 2007, 2008).

The projections to the CB have received minor attention. In this respect, labeling in a portion of the Tu was always accompanied by labeling of those CB adjacent to it (see **Table 3**) suggesting that the Tu and CB are functionally related.

FUNCTIONAL CONSIDERATIONS: ROLE OF AMYGDALO-STRIATAL PATHWAYS IN EMOTIONAL EVALUATION OF CHEMOSENSORY STIMULI

As we have seen, the pallial amygdala projects heavily to the core and shell of the nucleus accumbens, the olfactory tubercle, and the striatal cell bridges linking the ventral Acb with the Tu, and the ICj. The amygdalo-accumbens projection is considered to be involved in reward-related processes (Everitt et al., 1999; Baxter and Murray, 2002; see below). In this respect, our findings lead to two main conclusions.

First of all, the Tu receives massive projections from the pallial amygdala, conveying olfactory and vomeronasal information (from the cortical amygdala) and non-chemosensory information (from the basolateral amygdala). Since these projections mainly terminate in layers 2 and 3, they likely target the cell bodies and proximal dendrites of the principal cells and thus probably have a strong influence on the activity of the Tu. Therefore, the Tu, CB and ICj constitute a portion of the ventral striatum mediating responses to a variety of chemosensory and non-chemosensory stimuli, as suggested by Talbot et al. (1988a,b) on the basis of anatomical and neurochemical studies in different mammals. In this respect, several nuclei of the pallial amygdala project to the ICj. However, the projection from the COApm (the main cortical target of the accessory olfactory bulb, Scalia and Winans, 1975) apparently terminates, in a fairly specific way, in the neuropile-rich core of the ICj, and in the lateral aspect of the ICjM. Although the inner structure and cell composition of the ICj are very complex (Fallon et al., 1978, 1983; Fallon, 1983), the specific input from a vomeronasal relay suggest that some ICj might be specialized structures of the ventral striatum devoted to processing vomeronasal information.

The second conclusion drawn from our findings is that the medial Tu and adjoining structures (CB and ICj) are very likely involved in mediating (affective) reward-related responses to chemical signals. This is supported by the fact that both electrical stimulation in the medial Tu (Prado-Alcala and Wise, 1984) and local administration of addictive drugs (Kornetsky et al., 1991; Ikemoto et al., 2005) are rewarding. Since the medial aspect of the Tu and neighboring CB and ICj, including the ICjM, receive distinct projections from the vomeronasal amygdala (COApm and AHA) and stimulation of the vomeronasal amygdala is rewarding (Kane et al., 1991), it is likely that these amygdalo-striatal projections mediate reward responses to (among other stimuli) vomeronasal- and/or olfactory-detected chemosignals (see also Úbeda-Bañón et al., 2007, 2008).

Regarding the projections from the basolateral amygdala to the ventral striatum, they are involved in the expression of reward-related behaviors toward secondary reinforcers (Cador et al., 1989; Everitt et al., 1989). In fact, Pavlovian second-order conditioning is impaired by lesions of either the accumbens (Parkinson et al., 1999) or the basolateral amygdala (Hatfield et al., 1996; Blundell et al., 2001). These findings indicate that the learning processes occurring in the basolateral amygdala endow neutral stimuli with appetitive properties by means of their association with primary reinforcers. Through its projections to the ventral striatum, the basolateral amygdala would mediate goal-directed responses to these newly attractive stimuli.

In this respect, it has been shown in female mice that odorants are not innately attractive but become so after their association with non-volatile (e.g., vomeronasal), innately rewarding male pheromones (Moncho-Bogani et al., 2002; Martínez-Ricós et al., 2007, 2008; Roberts et al., 2010). This association of olfactory and vomeronasal stimuli might occur in the basolateral amygdala, since the cortical amygdala, and piriform cortex (present results; McDonald, 1998) display convergent projections to deep amygdaloid nuclei (Canteras et al., 1992; Pitkänen, 2000; Lanuza et al., 2008). This hypothesis is consistent with the expression of c-fos in the basolateral amygdala of female mice induced by male odors before and after olfactory–vomeronasal associative learning (Moncho-Bogani et al., 2005). A similar role has been proposed for the basolateral amygdala in olfactory–gustatory associative learning mediating go–no go appetitive responses (Schoenbaum et al., 1999).

EVOLUTION OF THE EMOTIONAL BRAIN

Comparative studies (Bruce and Neary, 1995; Martínez-García et al., 2002, 2007) indicate that reptiles possess a well-developed pallial amygdala composed of chemosensory cortical structures (superficial, layered) and multimodal deep nuclei. Anatomical and neurochemical data in different reptiles and in birds strongly suggest that the projections from the pallial amygdala to the ventral striatum were already present in the ancestral amniote and underwent a conservative evolution (Novejarque et al., 2004; Martínez-García et al., 2007). In this respect, our finding that parts of the cortical amygdala of mammals display substantial projections to the ventral striatum fit the results of similar studies in non-mammals. Thus, the vomeronasal cortex of squamate reptiles (the nucleus sphericus), like its mammalian counterpart, the COApm, projects massively to a portion of the ventral striatum located between the nucleus accumbens and the olfactory tubercle. In snakes this portion of the ventral striatum is called the olfactostriatum (Lanuza and Halpern, 1997), and displays characteristic neurochemical features (Martínez-Marcos et al., 2005). Together with recent data in rats (Úbeda-Bañón et al., 2008), the present results suggest that the "olfactostriatum" would be represented in the mammalian brain by the anteromedial cell bridges and ICj, plus portions of the adjacent Tu that receive the projection from the COApm. In fact, like the ophidian olfactostriatum (Martínez-Marcos et al., 2005) the medial portions of the CB, the ICj, and the Tu display a moderate-to-dense innervation of neuropeptide Y-immunoreactive fibers (Riedel et al., 2002; Úbeda-Bañón et al., 2008). In addition, cells in the Tu and the ICj express 5-hydroxytryptamine-2A receptors (Mijnster et al., 1997; Jansson et al., 2001). Although these data support this homology, it is noteworthy that the CB, the ICj, and the Tu show a

high density of TH-immunoreactive axons (Seifert et al., 1998; Riedel et al., 2002; Úbeda-Bañón et al., 2008), whereas the ophidian olfactostriatum displays a comparatively sparser innervation of TH-immunoreactive fibers (Martínez-Marcos et al., 2005).

Anatomical, neurochemical, and functional data suggest that the telencephalon of the ancestral amniote possessed an amygdalo-striatal system. The fact that this circuitry has remained well conserved indicates that its function is crucial for survival and reproduction. Indeed, the amygdala receives multimodal sensory information and controls the expression of basic emotional behaviors, namely reward/attraction (throughout its projections to ventral striatum) or fear/anxiety/aversion (throughout its projections to the central extended amygdala). Therefore, in the ancestral amniote, the amygdalo-striatal system constituted part of the primordial emotional brain, since it probably allowed not only the appropriate behavioral response toward unconditioned attractive (rewarding) stimuli, but also learning from these events by means of the emotional tagging of neutral sensory stimuli.

ACKNOWLEDGMENTS

Funded by the Spanish Ministry of Education and Science-FEDER (BFU2007-67912-C02-01/BFI and BFU2010-16656), Generalitat Valenciana (ACOMP/2010/127) and the Junta de Comunidades de Castilla-La Mancha (PEIC11-0045-4490).

REFERENCES

Aggleton, J. P. (ed.). (2000). *The Amygdala. A Functional Analysis*, 2nd Edn. Oxford: Oxford University Press.

Agustín-Pavón, C., Martínez-Ricós, J., Martínez-García, F., and Lanuza, E. (2007). Effects ofdopaminergic drugs on innate pheromone-mediated reward in female mice: a new case of dopamine-independent "liking". *Behav. Neurosci.* 121, 920–932.

Baxter, M. G., and Murray, E. A. (2002). The amygdala and reward. *Nat. Rev. Neurosci.* 3, 563–573.

Blundell, P., Hall, G., and Killcross, S. (2001). Lesions of the basolateral amygdala disrupt selective aspects of reinforcer representation in rats. *J. Neurosci.* 21, 9018–9026.

Brog, J. S., Salyapongse, A., Deutch, A. Y., and Zahm, D. S. (1993). The patterns of afferent innervation of the core and shell in the "accumbens" part of the rat ventral striatum: immunohistochemical detection of retrogradely transported fluoro-gold. *J. Comp. Neurol.* 338, 255–278.

Bruce, L. L., and Neary, T. J. (1995). The limbic system of tetrapods: a comparative analysis of cortical and amygdalar populations. *Brain Behav. Evol.* 46, 224–234.

Cador, M., Robbins, T. W., and Everitt, B. J. (1989). Involvement of the amygdala in stimulus-reward associations: interaction with the ventral striatum. *Neuroscience* 30, 77–86.

Caffé, A. R., van Leeuwen, F. W., and Luiten, P. G. (1987). Vasopressin cells in the medial amygdala of the rat project to the lateral septum and ventral hippocampus. *J. Comp. Neurol.* 261, 237–252.

Canteras, N. S., Simerly, R. B., and Swanson, L. W. (1992). Connections of the posterior nucleus of the amygdala. *J. Comp. Neurol.* 324, 143–179.

Everitt, B. J., Cador, M., and Robbins, T. W. (1989). Interactions between the amygdala and ventral striatum in stimulus-reward associations: studies using a second-order schedule of sexual reinforcement. *Neuroscience* 30, 63–75.

Everitt, B. J., Cardinal, R. N., Parkinson, J. A., and Robbins, T. W. (2003). Appetitive behavior: impact of amygdala-dependent mechanisms of emotional learning. *Ann. N. Y. Acad. Sci.* 985, 233–250.

Everitt, B. J., Morris, K. A., O'Brien, A., and Robbins, T. W. (1991). The basolateral amygdala-ventral striatal system and conditioned place preference: further evidence of limbic-striatal interactions underlying reward-related processes. *Neuroscience* 42, 1–18.

Everitt, B. J., Parkinson, J. A., Olmstead, M. C., Arroyo, M., Robledo, P., and Robbins, T. W. (1999). Associative processes in addiction and reward. The role of amygdala- ventral striatal subsystems. *Ann. N. Y. Acad. Sci.*877, 412–438.

Fallon, J. H. (1983). The islands of Calleja complex of rat basal forebrain II: connections of medium and large sized cells. *Brain Res. Bull.* 10, 775–793.

Fallon, J. H., Loughlin, S. E., and Ribak, C. E. (1983). The islands of Calleja complex of rat basal forebrain. III. Histochemical evidence for a striatopallidal system. *J. Comp. Neurol.* 218, 91–120.

Fallon, J. H., Riley, J. N., Sipe, J. C., and Moore, R. Y. (1978). The islands of Calleja: organization and connections. *J. Comp. Neurol.* 181, 375–395.

Friedman, D. P., Aggleton, J. P., and Saunders, R. C. (2002). Comparison of hippocampal, amygdala, and perirhinal projections to the nucleus accumbens: combined anterograde and retrograde tracing study in the Macaque brain. *J. Comp. Neurol.* 450, 345–365.

Fudge, J. L., Breitbart, M. A., and McClain, C. (2004). Amygdaloid inputs define a caudal component of the ventral striatum in primates. *J. Comp. Neurol.* 476, 330–347.

Fudge, J. L., Kunishio, K., Walsh, P., Richard, C., and Haber, S. N. (2002). Amygdaloid projections to ventromedial striatal subterritories in the primate. *Neuroscience* 110, 257–275.

Groenewegen, H. J., Becker, N. E., and Lohman, A. H. (1980). Subcortical afferents of the nucleus accumbens septi in the cat, studied with retrograde axonal transport of horseradish peroxidase and bisbenzimid. *Neuroscience* 5, 1903–1916.

Gutiérrez-Castellanos, N., Martínez-Marcos, A., Martínez-García, F., and Lanuza, E. (2010). Chemosensory function of the amygdala. *Vitam. Horm.* 83, 165–196.

Haga, S., Hattori, T., Sato, T., Sato, K., Matsuda, S., Kobayakawa, R., Sakano, H., Yoshihara, Y., Kikusui, T., and Touhara, K. (2010). The male mouse pheromone ESP1 enhances female sexual receptive behaviour through a specific vomeronasal receptor. *Nature* 466, 118–122.

Hatfield, T., Han, J. S., Conley, M., Gallagher, M., and Holland, P. (1996). Neurotoxic lesions of basolateral, but not central, amygdala interfere with Pavlovian second-order conditioning and reinforcer devaluation effects. *J. Neurosci.* 16, 5256–5265.

Ikemoto, S., Qin, M., and Liu, Z.-H. (2005). The functional divide for primary reinforcement of D-amphetamine lies between the medial and lateral ventral striatum: is the division of the accumbens core, shell, and olfactory tubercle valid? *J. Neurosci.* 25, 5061–5065.

Jansson, A., Tinner, B., Bancila, M., Verge, D., Steinbusch, H. W., Agnati, L. F., and Fuxe, K. (2001). Relationships of 5-hydroxytryptamine immunoreactive terminal-like varicosities to 5-hydroxytryptamine-2A receptor-immunoreactive neuronal processes in the rat forebrain. *J. Chem. Neuroanat.* 22, 185–203.

Johnston, J. B. (1923). Further contributions to the study of the evolution of the forebrain. *J. Comp. Neurol.* 35, 337–481.

Kane, F., Coulombe, D., and Miliaressis, E. (1991). Amygdaloid self-stimulation: a movable electrode mapping study. *Behav. Neurosci.* 105, 926–932.

Kelley, A. E., Domesick, V. B., and Nauta, W. J. H. (1982). The amygdalostriatal projection in the rat – an anatomical study by anterograde and retrograde tracing methods. *Neuroscience* 7, 615–630.

Kemppainen, S., Jolkkonen, E., and Pitkänen, A. (2002). Projections from the posterior corticalnucleus of the amygdala to the hippocampal formation and parahippocampal regionin rat. *Hippocampus* 12, 735–755.

Kornetsky, C., Huston-Lyons, D., and Porrino, L. J. (1991). The role of the olfactory tubercle in the effects of cocaine, morphine and brain-stimulation reward. *Brain Res.* 541, 75–81.

Krettek, J. E., and Price, J. L. (1978). Amygdaloid projections to subcortical structures within the basal forebrain and brainstem in the rat and cat. *J. Comp. Neurol.* 178, 225–254.

Lanuza, E., and Halpern, M. (1997). Afferent and efferent connections of the nucleus sphericus in the snake Thamnophis sirtalis: convergence of olfactory and vomeronasal information in the lateral cortex and the amygdala. *J. Comp. Neurol.* 385, 627–640.

Lanuza, E., Novejarque, A., Martínez-Ricós, J., Martínez-Hernández, J., Agustín-Pavón, C., and Martínez-García, F. (2008). Sexual pheromones and the evolution of the reward system of the brain: the chemosensory function of the amygdala. *Brain Res. Bull.* 75, 460–466.

LeDoux, J. E. (2000). Emotion circuits in the brain. *Annu. Rev. Neurosci.* 23, 155–184.

LeDoux, J. E., Cicchetti, P., Xagoraris, A., and Romanski, L. M. (1990). The lateral amygdaloid nucleus: sensory interface of the amygdala in fear conditioning. *J. Neurosci.* 10, 1062–1069.

Luskin, M. B., and Price, J. L. (1983). The topographic organization of associational fibers ofthe olfactory system in the rat, including centrifugal fibers to the olfactorybulb. *J. Comp. Neurol.* 216, 264–291.

Majak, K., and Pitkänen, A. (2003). Projections from the periamygdaloid cortex to theamygdaloid complex, the hippocampal formation, and the parahippocampal region: a PHA-L study in the rat. *Hippocampus* 13, 922–942.

Martínez-García, F., Martínez-Marcos, A., and Lanuza, E. (2002). The pallial amygdala of amniote vertebrates: evolution of the concept, evolution of the structure. *Brain Res. Bull.* 57, 463–469.

Martínez-García, F., Novejarque, A., and Lanuza, E. (2007). "Evolution of the amygdala in vertebrates"in *Evolution of Nervous Systems*, ed. J. H. Kaas (Oxford: Academic Press), 255–334.

Martínez-Hernández, J., Lanuza, E., and Martínez-García, F. (2006). Selective dopaminergic lesions of the ventral tegmental area impair preference for sucrose but not formale sexual pheromones in female mice. *Eur. J. Neurosci.* 24, 885–893.

Martínez-Marcos, A., Úbeda-Bañón, I., Lanuza, E., and Halpern, M. (2005). Chemoarchitecture and afferent connections of the "olfactostriatum": a specialized vomeronasal structure within the basal ganglia of snakes. *J. Chem. Neuroanat.* 29, 49–69.

Martínez-Ricós, J., Agustín-Pavón, C., Lanuza, E., and Martínez-García, F. (2007). Intraspecific communication through chemical signals in female mice: reinforcing properties of involatile male sexual pheromones. *Chem. Senses* 32, 139–148.

Martínez-Ricós, J., Agustín-Pavón, C., Lanuza, E., and Martínez-García, F. (2008). Role of the vomeronasal system in intersexual attraction in female mice. *Neuroscience* 153, 383–395.

McDonald, A. J. (1991a). Organization of amygdaloid projections to the prefrontal cortex and associated striatum in the rat. *Neuroscience* 44, 1–14.

McDonald, A. J. (1991b). Topographical organization of amygdaloid projections to the caudatoputamen, nucleus accumbens, and related striatal-like areas of the rat brain. *Neuroscience* 44, 15–33.

McDonald, A. J. (1998). Cortical pathways to the mammalian amygdala. *Prog. Neurobiol.* 55, 257–332.

Mijnster, M. J., Raimundo, A. G., Koskuba, K., Klop, H., Docter, G. J., Groenewegen, H. J., and Voorn, P. (1997). Regional and cellular distribution of serotonin 5-hydroxytryptamine 2a receptor mRNA in the nucleus accumbens, olfactory tubercle, and caudate putamen of the rat. *J. Comp. Neurol.* 389, 1–11.

Moncho-Bogani, J., Lanuza, E., Hernández, A., Novejarque, A., and Martínez-García, F. (2002). Attractive properties of sexual pheromones in mice. Innate or learned? *Physiol. Behav.* 77, 167–176.

Moncho-Bogani, J., Martínez-García, F., Novejarque, A., and Lanuza, E. (2005). Attraction to sexual pheromones and associated odorants in female mice involves activation of the reward system and basolateral amygdala. *Eur. J. Neurosci.* 21, 2186–2198.

Novejarque, A., Lanuza, E., and Martínez-García, F. (2004). Amygdalostriatal projections in reptiles: a tract-tracing study in the lizard Podarcis hispanica. *J. Comp. Neurol.* 479, 287–308.

Ottersen, O. P. (1982). Connections of the amygdala of the rat. IV: corticoamygdaloid andintraamygdaloid connections as studied with axonal transport of horseradishperoxidase. *J. Comp. Neurol.* 205, 30–48.

Parkinson, J. A., Olmstead, M. C., Burns, L. H., Robbins, T. W., and Everitt, B. J. (1999). Dissociation in effects of lesions of the nucleus accumbens core and shell on appetitive pavlovian approach behavior and the potentiation of conditioned reinforcement and locomotor activity by D-amphetamine. *J. Neurosci.* 19, 2401–2411.

Paxinos, G., and Franklin, K. B. J. (2001). *The Mouse Brain in Stereotaxic Coordinates*, 2nd Edn. San Diego: Academic Press.

Petrovich, G. D., Risold, P. Y., and Swanson, L. W. (1996). Organization of projections from the basomedial nucleus of the amygdala: a PHAL study in the rat. *J. Comp. Neurol.* 374, 387–420.

Pitkänen, A. (2000). "Connectivity of the rat amygdaloid complex"in *The Amygdala. A functional analysis*, 2nd Edn, ed. J. P. Aggleton (Oxford: Oxford University Press), 31–115.

Pitkänen, A., Savander, V., and Ledoux, J. E. (1997). Organization of intra-amygdaloid circuitries in the rat: an emerging framework for understanding functions of the amygdala. *Trends Neurosci.* 20, 517–523.

Prado-Alcala, R., and Wise, R. A. (1984). Brain stimulation reward and dopamine terminal fields. I. Caudate-putamen, nucleus accumbens and amygdala. *Brain Res.* 297, 265–273.

Price, J. L., Russchen, F. T., and Amaral, D. G. (1987). "The limbic region. II: the amygdaloid complex" in *Handbook of Chemical Neuroanatomy, Vol. 5, Integrated Systems*, eds T. Hökfelt, A. Björklund, and L. W. Swanson (Amsterdam: Elsevier), 279–338.

Puelles, L., Kuwana, E., Puelles, E., Bulfone, A., Shimamura, K., Keleher, J., Smiga, S., and Rubenstein, J. L. (2000). Pallial and subpallial derivatives in the embryonic chick and mouse telencephalon, traced by the expression of the genes Dlx-2, Emx-1, Nkx- 2.1, Pax-6, and Tbr-1. *J. Comp. Neurol.* 424, 409–438.

Rajakumar, N., Elisevich, K., and Flumerfelt, B. A. (1993). Biotinylated dextran: a versatile anterograde and retrograde neuronal tracer. *Brain Res.* 607, 47–53.

Reiner, A., Veenman, C. L., Medina, L., Jiao, Y., Del Mar, N., and Honig, M. G. (2000). Pathway tracingusing biotinylated dextran amines. *J. Neurosci. Methods* 103, 23–37.

Riedel, A., Hartig, W., Seeger, G., Gartner, U., Brauer, K., and Arendt, T. (2002). Principles of rat subcortical forebrain organization: a study using histological techniques and multiple fluorescence labeling. *J. Chem. Neuroanat.* 23, 75–104.

Robbins, T. W., Cador, M., Taylor, J. R., and Everitt, B. J. (1989). Limbic-striatal interactions in reward-related processes. *Neurosci. Biobehav. Rev.* 13, 155–162.

Roberts, S. A., Simpson, D. M., Armstrong, S. D., Davidson, A. J., Robertson, D. H., McLean, L., Beynon, R. J., and Hurst, J. L. (2010). Darcin: a male pheromone that stimulates female memory and sexual attraction to an individual male's odour. *BMC Biol.* 8, 75. doi: 10.1186/1741-7007-8-75

Russchen, F. T., Bakst, I., Amaral, D. G., and Price, J. L. (1985). The amygdalostriatal projections in the monkey. An anterograde tracing study. *Brain Res.* 329, 241–257.

Russchen, F. T., and Price, J. L. (1984). Amygdalostriatal projections in the rat. Topographical organization and fiber morphology shown using the lectin PHA-L as an anterograde tracer. *Neurosci. Lett.* 47, 15–22.

Santiago, A. C., and Shammah-Lagnado, S. J. (2004). Efferent connections of the nucleus of the lateral olfactory tract in the rat. *J. Comp. Neurol.* 471, 314–332.

Scalia, F., and Winans, S. S. (1975). The differential projections of the olfactory bulb and accessory olfactory bulb in mammals. *J. Comp. Neurol.* 161, 31–55.

Schoenbaum, G., Chiba, A. A., and Gallagher, M. (1999). Neural encoding in orbitofrontal cortex and basolateral amygdala during olfactory discrimination learning. *J. Neurosci.* 19, 1876–1884.

Schofield, B. R. (2008). Retrograde axonal tracing with fluorescent markers. *Curr. Protoc. Neurosci.* Chapter 1, Unit 1.17.

Schofield, B. R., and Cant, N. B. (1996). Origins and targets of commissural connections between the cochlear nuclei in guinea pigs. *J. Comp. Neurol.* 375, 128–146.

Seifert, U., Hartig, W., Grosche, J., Bruckner, G., Riedel, A., and Brauer, K. (1998). Axonal expression sites of tyrosine hydroxylase, calretinin- and calbindin-immunoreactivity in striato-pallidal and septal nuclei of the rat brain: a double-immunolabelling study. *Brain Res.* 795, 227–246.

Shammah-Lagnado, S. J., and Santiago, A. C. (1999). Projections of the amygdalopiriform transition area (APir). A PHA-L study in the rat. *Ann. N. Y. Acad. Sci.* 877, 665–660.

Swanson, L. W., and Petrovich, G. D. (1998). What is the amygdala? *Trends Neurosci.* 21, 323–331.

Talbot, K., Woolf, N. J., and Butcher, L. L. (1988a). Feline islands of Calleja complex: I. Cytoarchitectural organization and comparative anatomy. *J. Comp. Neurol.* 275, 553–579.

Talbot, K., Woolf, N. J., and Butcher, L. L. (1988b). Feline islands of Calleja complex: II. Cholinergic and cholinesterasic features. *J. Comp. Neurol.* 275, 580–603.

Turner, B. H., and Herkenham, M. (1991). Thalamoamygdaloid projections in the rat: a test of the amygdala's role in sensory processing. *J. Comp. Neurol.* 313, 295–325.

Úbeda-Bañón, I., Novejarque, A., Mohedano-Moriano, A., Pro-Sistiaga, P., de la Rosa-Prieto, C., Insausti, R., Martinez-Garcia, F., Lanuza, E., and Martinez-Marcos, A. (2007). Projections from the posterolateral olfactory amygdala to

the ventral striatum: neural basis for reinforcing properties of chemical stimuli. *BMC Neurosci.* 8, 103. doi: 10.1186/1471-2202-8-103

Úbeda-Bañón, I., Novejarque, A., Mohedano-Moriano, A., Pro-Sistiaga, P., Insausti, R., Martinez-Garcia, F., Lanuza, E., and Martinez-Marcos, A. (2008). Vomeronasal inputs to the rodent ventral striatum. *Brain Res. Bull.* 75, 467–473.

Wright, C. I., Beijer, A. V. J., and Groenewegen, H. J. (1996). Basal amygdaloid complex afferents to the rat nucleus accumbens are compartmentally organized. *J. Neurosci.* 16, 1877–1893.

Conflict of Interest Statement: The authors declare that the research was conducted in the absence of any commercial or financial relationships that could be construed as a potential conflict of interest.

Received: 20 June 2011; paper pending published: 08 July 2011; accepted: 03 August 2011; published online: 22 August 2011.

Citation: Novejarque A, Gutiérrez-Castellanos N, Lanuza E and Martínez-García F (2011) Amygdaloid projections to the ventral striatum in mice: direct and indirect chemosensory inputs to the brain reward system. Front. Neuroanat. ***5****:54. doi: 10.3389/fnana.2011.00054*